OPTIMIZATION OF VEHICLE DYNAMICS FOR ENHANCED CLASS 8 TRUCK PLATOONING

A Thesis

Submitted to the Faculty

of

Purdue University

by

Brady T. Black

In Partial Fulfillment of the

Requirements for the Degree

of

Master of Science in Mechanical Engineering

December 2020

Purdue University

West Lafayette, Indiana

THE PURDUE UNIVERSITY GRADUATE SCHOOL
STATEMENT OF THESIS APPROVAL

Dr. Gregory M. Shaver, Chair

School of Mechanical Engineering

Dr. Christopher S. Goldenstein

School of Mechanical Engineering

Dr. Peter H. Meckl

School of Mechanical Engineering

Approved by:

Dr. Nicole L. Key

Head of the School Graduate Program

Dedicated to my people of the Confederated Tribes of the Colville Reservation

ACKNOWLEDGMENTS

As I sit here late at night writing this final section before I deposit my thesis, I can't help but be overwhelmed with gratitude for everyone who has brought me to this point. I would not be where I am today if it wasn't for everyone who has helped me, supported me, and guided me to this point in my life.

First and foremost, my parents, Brett and Shelly Black. Thank you for raising me in a loving and nurturing home in which I was encouraged to thrive. I am so thankful that you gave me the freedom and support to pursue my passions.

To my high school guidance counselor, Dr. Susanna Hayes, thank you for believing in me when the statistics would have indicated that I would not succeed. Thank you for encouraging me to challenge myself and pursue graduate school when the world thought I would never even earn a Bachelor's Degree.

To my Stanford advisor, Professor Chris Edwards, thank you for allowing me, an eager and persistent undergraduate, to spend my sophomore summer in your lab. Thank you for bringing me back to spend a second summer after my senior year in your lab and giving me the literal keys to one of your test engines. And lastly, thank you for writing me a letter of recommendation for graduate school. It undoubtedly had a large impact on my acceptances, and I am incredibly grateful.

Michele Lezama, you told me that I would go to Purdue, and that I was not going to pay for it. Thank you for literally taking me by the arm and walking me around the entire AISES conference to help me apply to graduate school.

Thank you, Professor Greg Shaver, for taking me on as a graduate student in your lab. I am thankful that you decided to take a chance on me, and I hope that I have not disappointed you. You have given me the opportunity to work on a wide variety of problems, far more than any master's student could ever hope to have. I've really

enjoyed all the experiences I've had running the test cell, developing algorithms, and driving a class 8 truck. I think I can conclusively say that I have "drank the Koolaid."

Thank you to my friends for keeping me sane and grounded. Mark Berger and Ben Jensen for reminding me that there is a light at the end of the tunnel. Jesse Adkins for the countless phone calls. Chris Cameron for helping me apply to graduate school.

I would now like to take a moment to recognize everyone I have had the pleasure of working with in the Cummins Power Lab. Dr. Alex Taylor for the mentorship as I entered graduate school. Dr. Cody Allen for all of your assistance with the test cell. Ife Ibitayo for your never-ending patience and many, many post-graduation calls. John Foster, Shubham Ashta, and Miles Droege for being the best teammates a guy could ask for and also helping me with my thesis. Shveta Dhamankar for consistently schooling me at school. Jon Ore for always carving out time to help me with literally anything. Ryan Thayer for being the big brother I never had. And Julia Sibley for always making me laugh and feel welcomed.

The Sloan and the NAECC staff: Kevin Gibson, Felica Ahasteen-Bryant, Deb Swihart, and all other affiliated faculty. Thank you for supporting me through my graduate studies and for building a native community for me to lean on.

I would like to thank my lovely wife, Katherine Black. Thank you for supporting me pursuing this crazy path when it meant that we would be doing long distance for two years. I know the past two years have been challenging, but I sincerely believe that they have paid off, and I cannot wait to begin my happily ever after with you.

Last, but most importantly, I would like to thank God because He brought me through it all.

PREFACE

The work done in this thesis was done as a part of the DOE sponsored NEXTCAR (Next-Generation Energy Technologies for Connected and Automated On-Road Vehicles) project. Purdue's project title was "Connected and Automated Class 8 Trucks". In collaboration with two corporate partners: Cummins and Peloton Technology. The project goal was to enable an additional 20% reduction in energy consumption of future connected and automated freight trucks. The plan was to achieve this through: i) connectivity-enabled remote powertrain calibration, ii) connectivity-enabled, real-time powertrain control from the cloud, and iii) more efficient two-truck platooning using connectivity-enabled shifting coordination and lead truck predictive cruise control.

TABLE OF CONTENTS

Page

LIST OF TABLES

LIST OF FIGURES

Figure Page

SYMBOLS

A	state matrix
$\bar{A}$	frontal area of vehicle
B	input matrix
B_θ, f	follow vehicle grade input matrix
B_θ, p	preceding vehicle grade input matrix
$C_{D,0}$	nominal drag coefficient
d	distance between preceding and follow vehicle
d_{des}	desired vehicle separation
d_{max}	maximum vehicle separation
d_{min}	minimum vehicle separation
f	rolling resistance friction coefficient
F_{brake_f}	brake force of follow vehicle
F_{brake_p}	brake force of preceding vehicle
$F_{drag,f}$	drag force of follow vehicle
$F_{drag,p}$	drag force of preceding vehicle
$F_{gravity,f}$	gravity force of follow vehicle
$F_{gravity,p}$	gravity force of preceding vehicle
$F_{motive,f}$	engine force of follow vehicle
$F_{motive,p}$	engine force of preceding vehicle
$F_{roll,f}$	rolling resistance force of follow vehicle
$F_{roll,p}$	rolling resistance force of preceding vehicle
g	acceleration due to gravity
k	discrete time unit
m_f	mass of follow vehicle

m_p	mass of preceding vehicle
$m_{e,f}$	inertial mass of follow vehicle
$m_{e,p}$	inertial mass of preceding vehicle
N	horizon length
$P_{brake,f}$	brake power of follow vehicle
$P_{brake,f,com}$	commanded brake power of follow vehicle
$P_{brake,p}$	brake power of preceding vehicle
$P_{brake,p,com}$	commanded brake power of preceding vehicle
$P_{brake,max}$	maximum brake power
$P_{e,f}$	engine power of follow vehicle
$P_{e,f,com}$	commanded engine power of follow vehicle
$P_{e,max}$	maximum engine power
$P_{e,min}$	maximum retarder power
$P_{e,p}$	engine power of preceding vehicle
$P_{e,p,com}$	commanded engine power of preceding vehicle
$\dot{P}_{e,f}$	rate of change of engine power of follow vehicle
$\dot{P}_{e,max}$	maximum rate of change of engine power
$\dot{P}_{e,min}$	minimum rate of change of engine power
$\dot{P}_{e,p}$	rate of change of engine power of preceding vehicle
$\ddot{P}_{e,f}$	second derivative of engine power for follow vehicle
$\ddot{P}_{e,max}$	maximum value for second derivative of engine power
$\ddot{P}_{e,min}$	minimum value for second derivative of engine power
$\ddot{P}_{e,p}$	second derivative of engine power for preceding vehicle
p_0	y-intercept of drag coefficient linearization for follow vehicle
p_1	slope of drag coefficient linearization for follow vehicle
p_2	y-intercept of drag coefficient linearization for preceding vehicle
p_3	slope of drag coefficient linearization for preceding vehicle
u	input vector
S_f	position of the follow vehicle

S_p	position of the preceding vehicle
t_{final}	final time instance
t_{max}	maximum time to finish route
V_f	velocity of the follow vehicle
V_p	velocity of the preceding vehicle
$V_{p,des}$	desired velocity of the preceding vehicle
$\bar{V}$	mean velocity of the preceding and follow vehicles over the route
x	state vector
ρ	air density
θ_f	follow vehicle grade
θ_p	preceding vehicle grade
τ_b	brake constant
τ_e	engine constant

ABBREVIATIONS

AC	Alternating Current
ACC	Adaptive Cruise Control
BSFC	Brake Specific Fuel Consumption
CAN	Controller Area Network
DOE	Department of Energy
GHG	Greenhouse Gas
GPS	Global Positioning System
GVW	Gross Vehicle Weight
HD-FTP	Heavy-Duty Federal Test Procedure
I-280	Interstate 280
I-69	Interstate 69
LHPCC	Long-Horizon Predictive Cruise Control
MPC	Model Predictive Control
MPH	Miles Per Hour
NEXTCAR	Next-Generation Energy Technologies for Connected and Automated On-Road Vehicles
NREL	National Renewable Energy Laboratory
PECU	Peloton Engine Control Unit
PI	Proportional-Integral
PID	Proportional-Integral-Derivative
PP	PlatoonPro
ROGG	Route Optimized Gap Growth
SAE	Society of Automotive Engineers
SARS-CoV-2	Severe Acute Respiratory Syndrome Coronavirus 2

SS	Simultaneous Shifting

GLOSSARY

cut-ins	when a passenger vehicle drives in the gap between two platooning vehicles
dissolved platoon	the canceling of a platoon
HD-FTP	a drive cycle used for regulatory emission testing of heavy-duty on-road engines in the United States
J1321 Type II	a method for testing improvements in fuel economy set forth by the Society of Automotive Engineers
max droop	Cummins cruise controller droop settings are +3.1/-6.1 MPH
no droop	Cummins cruise controller droop settings are ± 0 MPH
platooning	drafting vehicles safely to save fuel
PlatoonPro	a sophisticated platooning controller developed by Peloton Technology
speed/torque profile	a file that is loaded into the dynamometer controller to command both engine speed and engine torque as functions of time
simultaneous shifting	commanding the follow vehicle in a platoon to shift at the same instance that the lead vehicle does
velocity profile	a file that is loaded into the vehicle to command vehicle velocity as a function of GPS location

ABSTRACT

Black, Brady T. M.S., Purdue University, December 2020. Optimization of Vehicle Dynamics for Enhanced Class 8 Truck Platooning. Major Professor: Gregory M. Shaver.

The heavy duty transportation sector is projected to grow in the coming decades. Increasing the fuel economy of class 8 vehicles would simultaneously decrease CO_2 emissions and decrease the annual fuel expenditures that account for nearly a quarter of cargo companies' annual budgets. Most technology that has aimed to do this has primarily been focused on either improvements in engine efficiency or reduction of aerodynamic drag. This thesis addresses a somewhat different approach: the optimization of vehicle dynamics in order to realize fuel savings.

Through partnerships with Peloton Technology and Cummins, tests and simulations were conducted on corridors with grades up to 5% that indicate fuel savings of up to 14.4% can be achieved through the combination of three strategies: two-truck platooning, long-horizon predictive cruise control (LHPCC), and simultaneous shifting. Two-truck platooning is the act of drafting a rear truck behind a front truck. It has been shown that this not only reduces the drag of the follow vehicle, but also that of the lead vehicle. LHPCC is an optimization of the lead truck's velocity over a given corridor to get "from point A to point B" in the most efficient way possible whilst doing so with a trip time constraint. Last is the use of simultaneous shifting, which allows the follow vehicle to maintain the proper platoon gap distance behind the lead truck.

1. INTRODUCTION

1.1 Motivation

With ever growing concerns about rising CO_2 levels in the atmosphere and an increasing interest in reducing the cost of operating a commercial vehicle fleet, there is great incentive for both the government as well as the heavy-duty vehicle industry to reduce the fuel consumption of commercial vehicles. Both the population and the per capita income of the world are continuing to grow. With this growth comes a rise in the demand for goods and services, and thus an increase in need for commercial transportation. Commercial vehicles not only comprise a large portion of the current global transportation sector's energy demand, but in the ExxonMobile 2019 Outlook for Energy, the increase of the heavy-duty sector is predicted to account for over 50% of the growth in energy demand from 2017 to 2040 [1]. A breakdown of the global transportation energy demand by sector is shown in Figure 1.1.

The heavy-duty transportation sector is not just a major part of the economy globally, but also in the United States. The entire transportation sector accounts for 28% of the greenhouse gas emissions in the United States, which is the sector with the highest greenhouse gas emissions in the nation [2]. Within the transportation sector, heavy-duty and medium-duty vehicles account for the second highest emissions after light-duty vehicles [3]. However, while light-duty vehicles trend toward hybridization and electrification, heavy-duty trucks struggle to make the transition due to the long periods of time that they are operated and the low energy density that currently plagues battery technology. Figure 1.2 shows the complete breakdown of greenhouse gas emissions by sector, and Figure 1.3 shows a further breakdown of greenhouse gas emissions within the transportation sector.

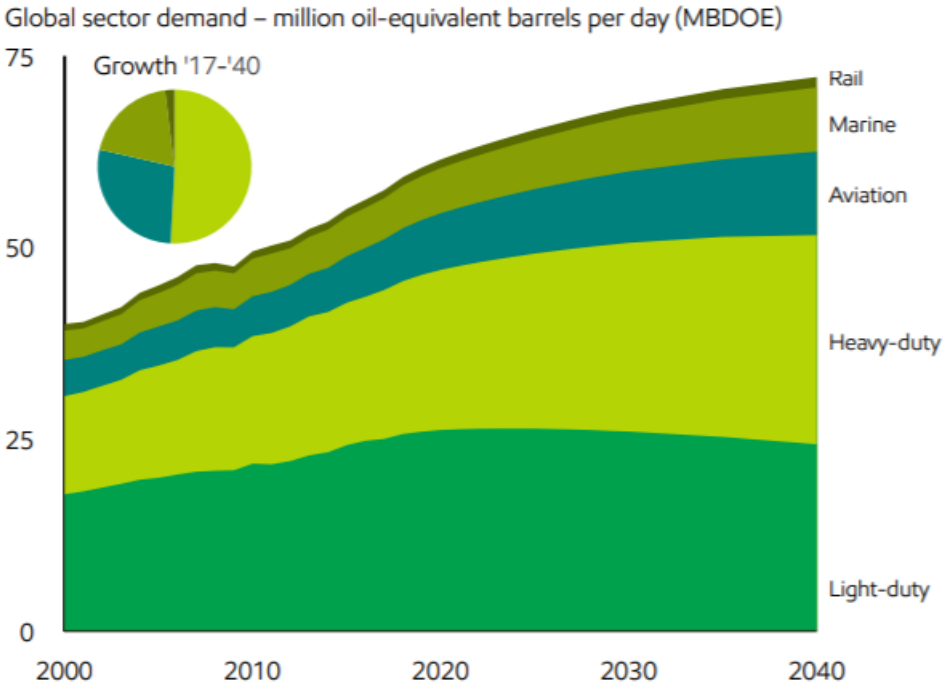

Fig. 1.1. Global Transportation Energy Demand [1]

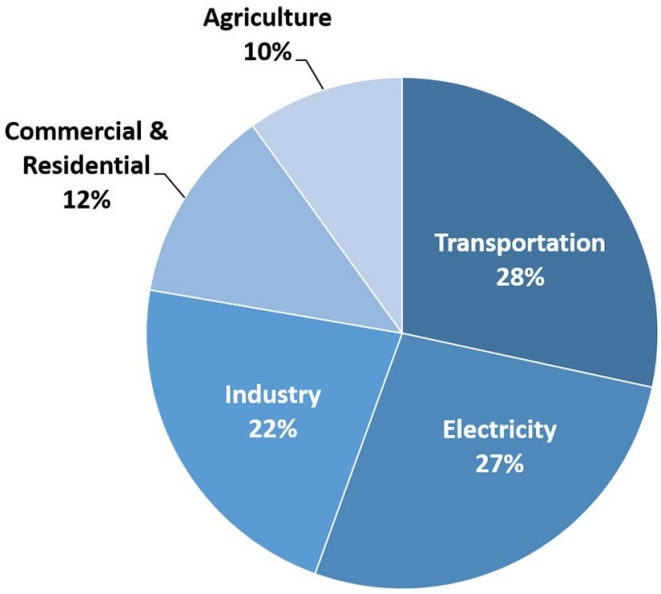

Fig. 1.2. Sources of Greenhouse Gas Emissions in 2018 [2]

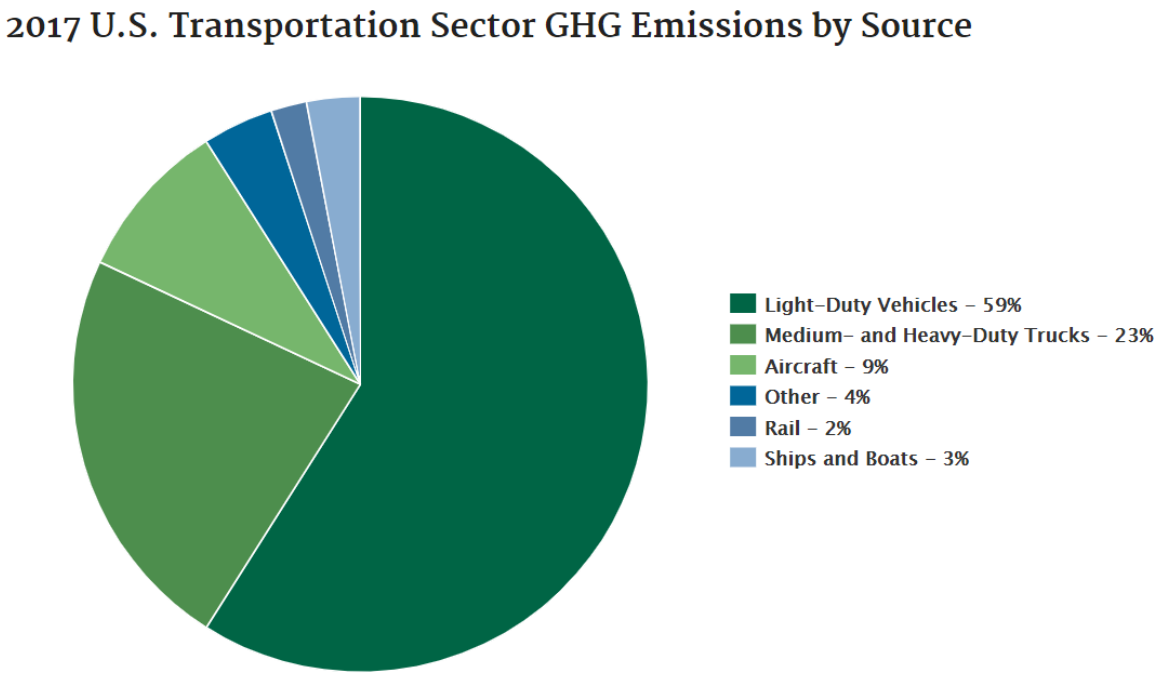

Fig. 1.3. U.S. Transportation Sector GHG Emissions by Source 2017 [3]

Class 8 trucks drive more miles per vehicle than any other vehicle in the U.S. Additionally, in the U.S., class 8 trucks consume the second highest amount of fuel per vehicle after transit buses [4]. However, there is over an order of magnitude more class 8 trucks than transit buses in the U.S., and transit bus operation yields itself better to hybridization or full electrification. A breakdown of average number of miles traveled by major vehicle category is shown in Figure 1.4, and a breakdown of average amount of fuel used on a yearly basis by vehicle type is shown in Figure 1.5.

As previously mentioned, there is not just an interest in reducing fuel consumption to reduce the greenhouse gas emissions of heavy-duty vehicles, but also to reduce fuel costs. A breakdown of the costs of a class 8 truck in the United States reveals that fuel is the second largest expense, after driver wages, to operate a truck [5]. Small improvements in the fuel economy of a class 8 vehicle can yield large monetary savings in operating costs of a fleet of class 8 trucks, and therefore lead to fleet operating

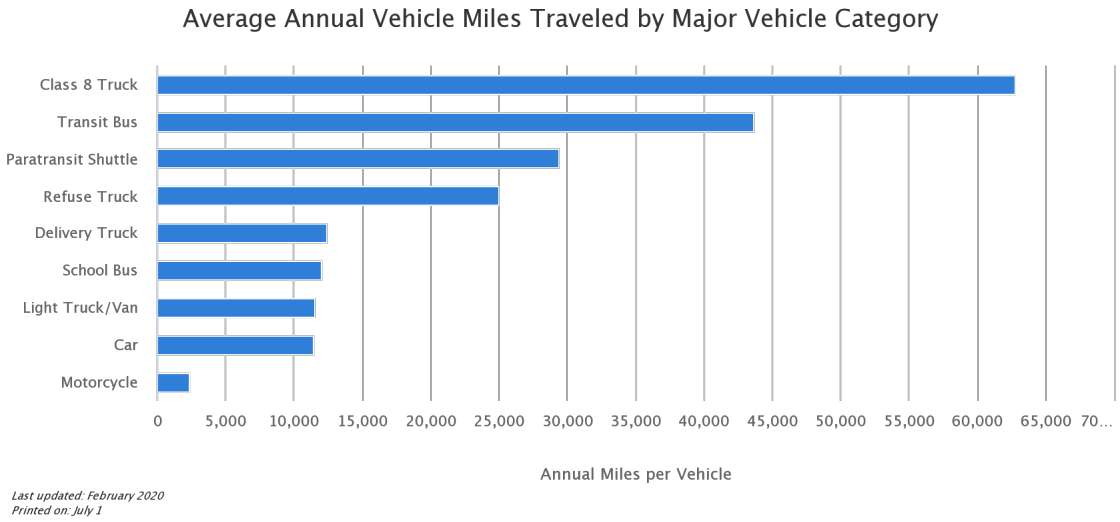

Fig. 1.4. Average Annual Vehicle Miles Traveled by Major Vehicle Category [4]

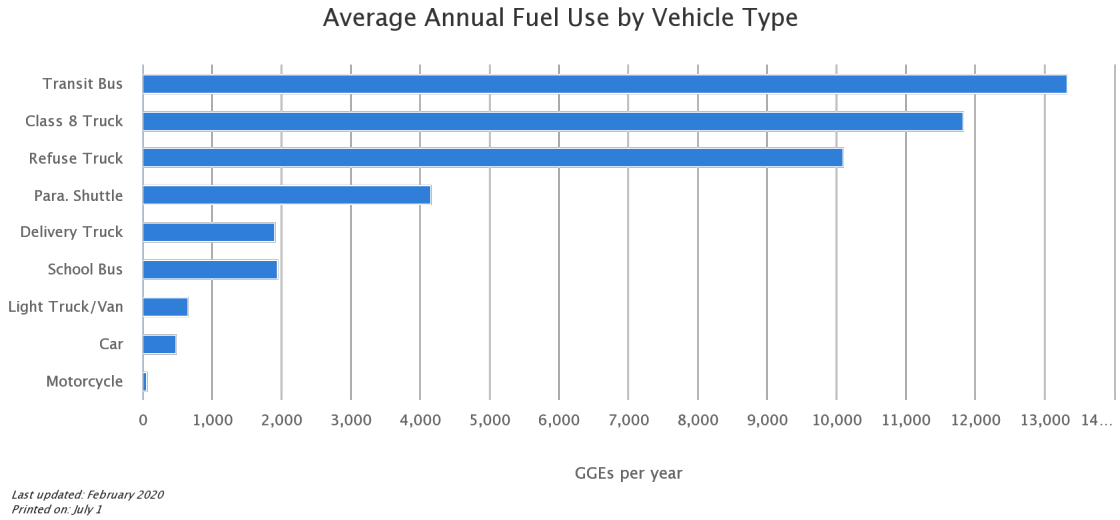

Fig. 1.5. Average Annual Fuel Use Per Vehicle by Vehicle Type [4]

companies improving their profit margins. A pie chart for major truck operating expenses is shown in Figure 1.6.

Lastly, the state of Indiana has a large interest in reducing the impact of trucking on the environment. Indiana is one of the few states where the majority of freight movement is not entering, leaving, or within the state. The majority of freight move-

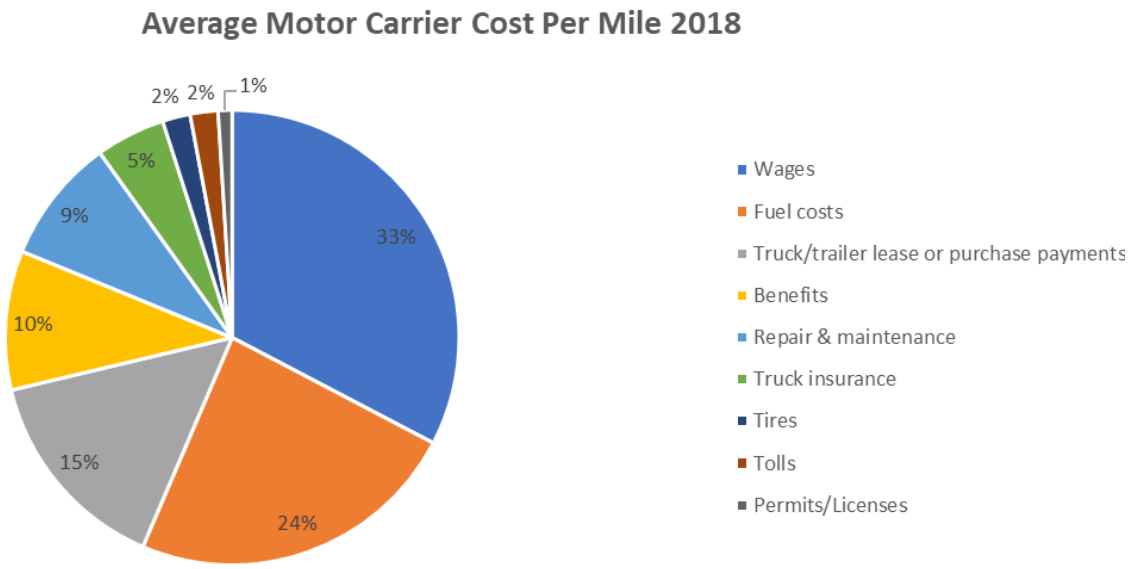

Fig. 1.6. Average Motor Carrier Cost Per Mile 2018 [5]

ment in Indiana is passing through the state, and this is expected to grow in the coming years [6]. A graphic of state to state truck flows using Indiana corridors for data from 2011 with a projection to 2040 is shown in Figure 1.7.

Class 8 trucks are a significant contributor to global climate change, and their usage is expected to grow in the coming decades. There is great interest in reducing their fuel consumption, which would, in turn, reduce their operating costs and reduce their carbon footprint. New and creative technologies are needed to address this problem.

1.2 Background

One of the major areas of inefficiencies in a class 8 vehicle comes from aerodynamic losses. Figure 1.8 shows that 22.3% of the vehicle's fuel energy goes into overcoming aerodynamic losses [7]. This is why low-clearance air dams, wheel covers, drive wheel fairings, trailer skirts, roof wind deflectors, trailer boat tails (etc.) have become

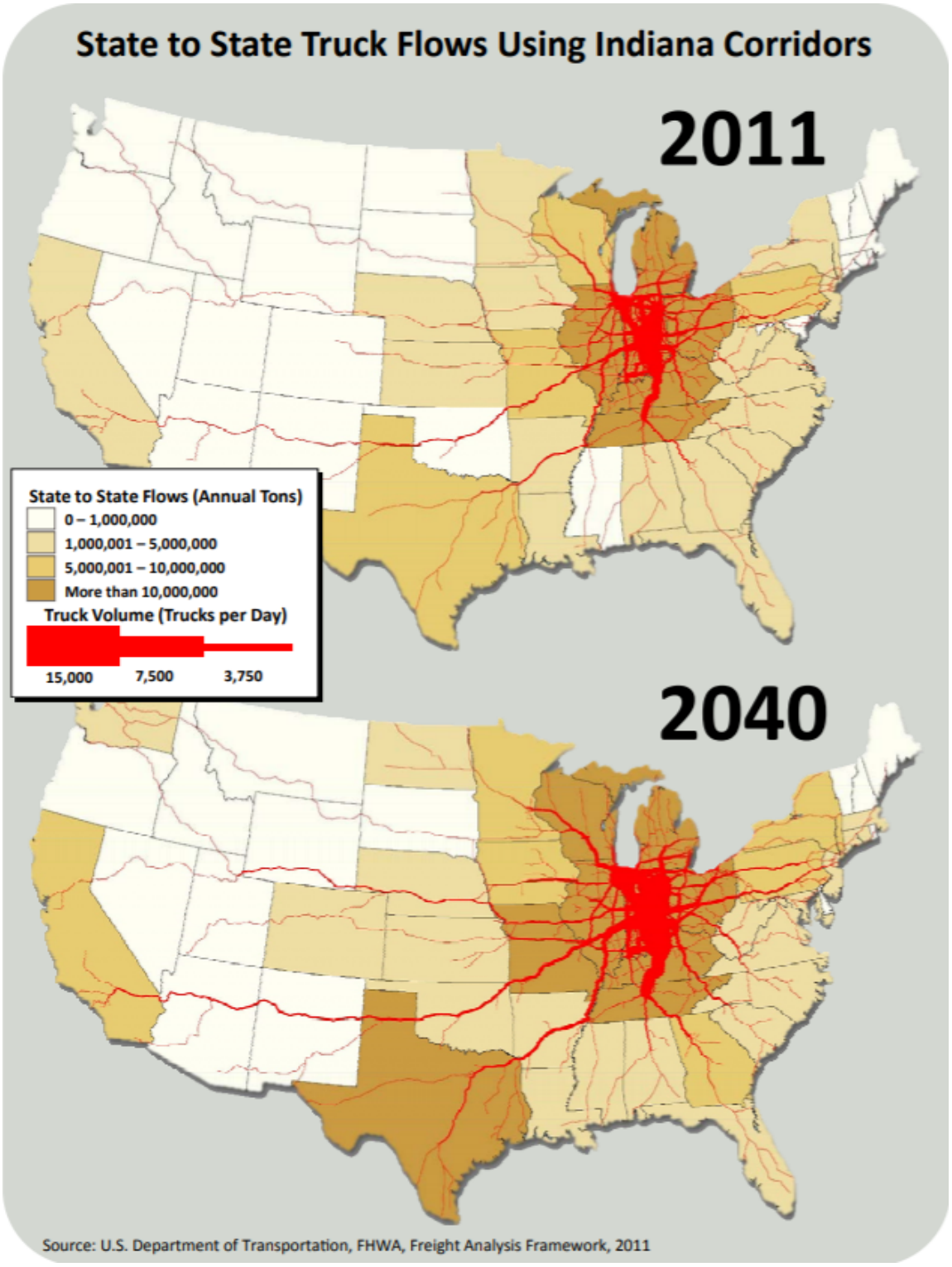

Fig. 1.7. State to State Truck Flows Using Indiana Corridors [6]

increasingly common. These devices are so effective that, in combination, one report states that "fleet owners who install gap fairings, side skirts and boat tails on their trucks can increase their fuel efficiency by 14% or more" [8].

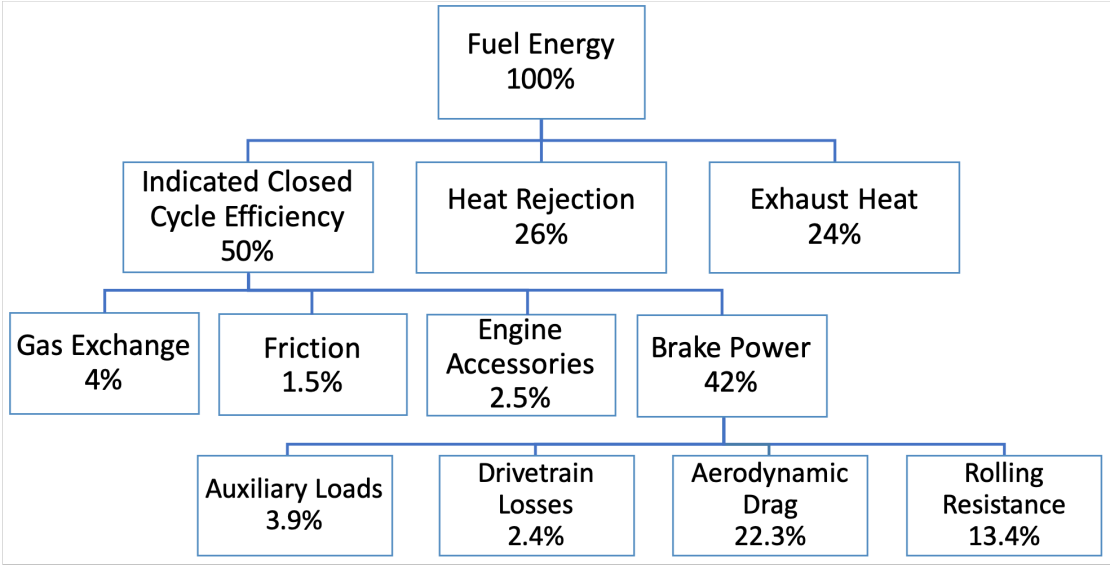

Fig. 1.8. Energy Balance of a Fully Loaded Class 8 Tractor-Trailer on a Level Road at 65 mph [7]

Platooning is another strategy that aims to reduce the aerodynamic drag force on vehicles by drafting one vehicle behind another. Figure 1.9 shows how not only the rear truck, but also the lead truck, experience a reduction in aerodynamic drag [9]. The rear truck, of course, sees a greater reduction in drag due to the lead truck displacing the air for the rear truck yielding reduced forebody drag. Furthermore, the lead truck also has some aerodynamic benefit due to the follow truck reducing the low pressure region behind the lead truck through the reduction of turbulence, thus reducing the pressure drag.

For the lead truck, a closer platoon gap appears to always yield more fuel savings. The follow truck follows this trend up to around a 50 foot gap, but then appears to loose some savings due to the cooling fans needing to turn on for proper airflow through the radiator [10]. Interestingly enough, the National Renewable Energy Lab-

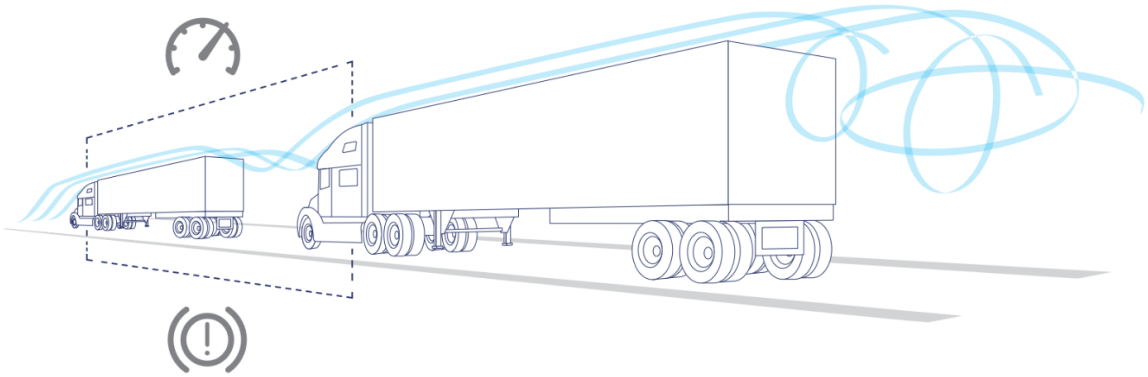

Fig. 1.9. Visualization of Airflow Over Two Platooning Class 8 Trucks [9]

oratory (NREL) also found that savings due to platooning appeared to be synergistic with aerodynamic improving features on trailers, i.e., trucks pulling trailers with aerodynamic improving features saved more fuel (during platooning) than trucks pulling trailers without aerodynamic improving features [10]. In order to safely drive class 8 trucks at 65 MPH at such short distances, Peloton claims that vehicle to vehicle communication is required [11]. Figures 1.10, 1.11, and 1.12, illustrate how vehicle to vehicle communication is necessary in order to safely close the platoon gap between two platooning vehicles.

Fig. 1.10. Driver Lag [11]

Fig. 1.11. Radar Lag [11]

Peloton states that their fixed gap platooning cuts fuel consumption by 4.5% on the lead truck and 10% on the follow truck for a platoon average of 7.25% savings [11].

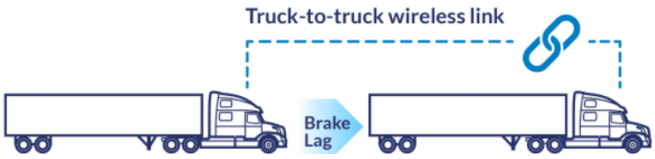

Fig. 1.12. PlatoonPro [11]

A separate study, led by NREL, found that on the Continental Proving Grounds in Uvalde, Texas, savings of up to 6.4% were measured using SAE J1321 Type II fuel testing standards [12].

A European study found that for a particular fleet, approximately 40% of all miles traveled could be in a platooning state [13]. Another study led by NREL showed that for the trucks across the U.S. for which they could confirm vehicle speed, 55.7% of miles traveled could be in a platooning state [14]; however, it should be noted that road grade was not a factor in this calculation, and it would likely prevent some of the miles from being platoonable by class 8 trucks. Furthermore, Peloton claims that in their trials, more than 80% of the platoonable miles have been utilized [15].

Significantly reducing the fuel consumption of class 8 trucks is a challenging task, but platooning appears to be a promising technology to reduce fuel consumption in class 8 vehicles.

1.3 Literature Review

The aim of the NEXTCAR project is to improve the performance of platooning, specifically on hilly terrain. Currently, platooning has primarily been implemented over flat and lightly graded corridors, as hilly terrain can result in excessive follow truck gap growth. While a respectable percentage of the U.S. roadways that class 8 trucks use fall into this category, increasing the number of roadways that trucks are able to platoon on would greatly increase the impact of this technology. Additionally, optimizing vehicle operation over various corridors could also lead to additional fuel savings above those obtained from platooning.

One simple strategy to help class 8 trucks maintain the gap on graded routes, proposed by Ibitayo, is to simultaneously shift the rear truck with the front truck [16]. Ibitayo shows that when simultaneous shifting is used, the maximum platoon gap over a section of Interstate 69 in Indiana is reduced from 34.3 meters to 20.5 meters. Management of gap is incredibly important because large platoon gaps can encourage cars to drive in between platooning vehicles (often referred to as a cut-in). Cut-ins demand the platoon to be canceled (also called "dissolved"). While simultaneous shifting appears to be a promising strategy to minimize and maintain platoon gap on aggressively graded roads and thus expand the number of miles where platooning is accessible to class 8 trucks, it currently does not show additional fuel savings over standard platooning [16].

Another successful strategy proposed by Ibitayo allows the rear truck to follow a variable gap profile, instead of a fixed gap, behind the lead truck. Foster took this concept and was able to successfully implement a PID style controller for the rear truck to track the optimized gap profiles [17]. Both Ibitayo and Foster report rear truck fuel savings of around 6-12% from a single-truck constant velocity baseline, and they show significantly lower maximum gap growths than when the rear truck was tracking a fixed gap. Lastly, operating the lead truck in a manner that is easier to follow by the rear truck appears to aid in the management of gap growth.

1.4 Thesis Outline

This chapter outlined the motivation for why fuel saving technologies for class 8 trucks are important. There is a high impact of class 8 trucks on the environment, and there are also cost saving benefits to be had through the reduction of fuel consumption of class 8 trucks. Furthermore, the chapter set forth a rationale for why aerodynamic improvements on class 8 trucks are a strong approach for saving fuel. It then delved into platooning as a promising technology for saving fuel, and then

addressed some of the challenges of platooning and some currently proposed solutions to those challenges.

Chapter 2 will discuss the use of an engine test cell as a means of obtaining a real-world estimate of fuel consumption before vehicle testing is conducted. It will also present some data of Purdue's fuel saving strategies that were previously run in simulation.

Chapter 3 will describe the framework developed for an MPC controller that was used to calculate the optimal velocity profile for a lead truck and the optimal gap profile for a follow truck (behind aforementioned lead truck) over two corridors in the United States. The chapter also shows the model being exercised through variations of parameters and constraints to learn more about the optimal profiles that were calculated.

Chapter 4 will discuss on-road testing that was conducted over a section of Interstate 69 in Indiana, and the subsequent data analysis. It also goes over predictions of truck behavior and fuel consumption of a high-fidelity vehicle model using the real-world data that was collected.

Chapter 5 will provide a summary of the work outlined in this thesis, emphasizing key conclusions, as well as proposing recommendations for future work.

2. TEST CELL REPEATABILITY

2.1 Motivation

While the focal point of this thesis is undoubtedly on simulations and on-road testing, an important part of the process of moving from the simulation space into on-road vehicle testing is the intermediate step of running an engine test cell. The engine test cell allows for a vehicle control strategy feasibility check, whereby it is possible to ensure that the engine speed and torque profiles are viable for the engine to follow (e.g., commanded changes are not faster than what the engine is able to respond to). Additionally, an engine test cell simultaneously acts as a fuel consumption calculator, in which real-world fuel consumption can be measured instead of relying upon simulation fuel consumption predictions. A high-fidelity vehicle model was developed with a powertrain (engine + transmission) "blackbox", from Cummins, that gives a predicted fuel consumption by Dr. Alexander Taylor [18]. The test cell can then verify the accuracy of these simulation predictions, which gives insight into the quantity of fuel that an on-road vehicle would consume. Lastly, the test cell can verify other model predictions, such as emissions, and ensure that a given vehicle control strategy does not increase emissions (particularly NO_x) over its respective baseline.

One important difference to note between the test cell and the Peterbilt 579 trucks (used for vehicle testing) is that the engine testbed was fed engine speed/torque profiles, but the on-road vehicles were fed a velocity setpoint as a function of GPS location. This will pose some discrepancy in the testbed fuel consumption vs. the vehicle fuel consumption. However, the conducted vehicle tests (discussed in Chapter 4), showed that the measured engine speed and torque from the on-road vehicle aligned very closely with the high-fidelity vehicle model simulation prediction over the same corridor.

Comparison of fuel consumption took on the order of hours in the simulation space and on the order of weeks when doing full J1321 Type II fuel tests with platooning vehicles (due to the strict requirements of ambient conditions as well as a lengthy vehicle pre-drive and warm-up procedure). The beauty of the test cell lies in its ability to generate real-world results on the order of days, and depending on the length and types of tests being conducted, as little as a single day. While this chapter will outline the number of tests that were run to ensure statistical significance and therefore repeatability, what was found, and what will be shown, is that there is value in as little as a single test for each strategy.

2.2 Experimental Setup and Testing Procedure

Inside Purdue's Herrick Laboratories Test Cell #2 is a Cummins X15 Efficiency Series shown in Figure 2.1. The engine is rated for 450 horsepower and 1750 foot-pounds of torque. The X15 is mated to a 670 horsepower Power Test AC dynamometer. Data was acquired via a Speedgoat real-time target machine, which runs on Simulink. Fuel consumption was calculated by gravimetric analysis through the use of a fuel container suspended by a load cell with before and after mass measurements taken for each test.

In order to ensure repeatable results, tests where fuel consumption data was needed were run only when the engine was in a "hot" state. A day of testing would begin with a heavy-duty federal test procedure (HD-FTP) to warm up the engine for the first test of the day, and all subsequent tests would be run after each other.

2.3 Routes of Interest

The focus of this thesis revolves around two main corridors of interest: Interstate 69 in southern Indiana and Interstate 280 in northern California. Two of the three parties involved with the NEXTCAR project reside in the state of Indiana (Purdue and Cummins), and the third resides in California (Peloton Technology). Because the

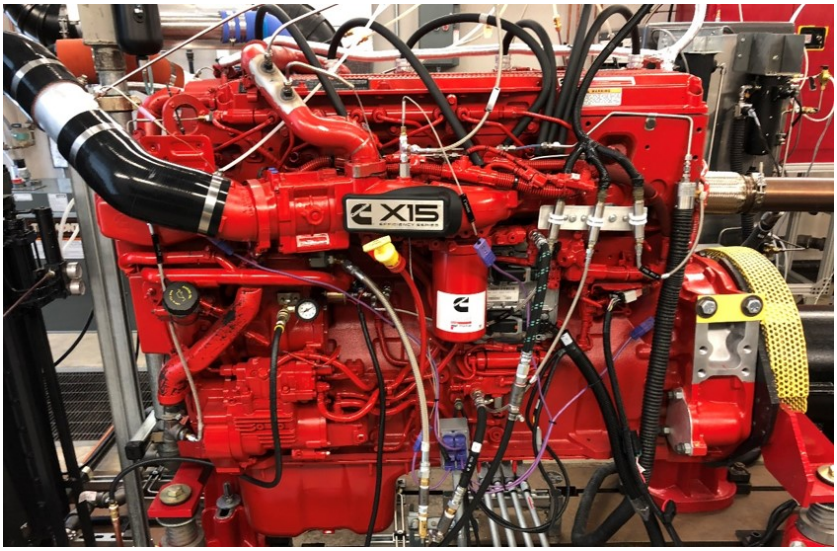

Fig. 2.1. Cummins X15

technology this thesis presents yields the greatest fuel savings over aggressively graded corridors, the most aggressive corridors that could be found within a reasonable distance of all parties involved were sought after. Both Interstate 69 and Interstate 280 were identified as corridors with grades that reach as high as 5%, and can be accessed by the parties in their respective states within a reasonable drive time.

2.3.1 Interstate 69

Interstate 69 runs south to north through the state of Indiana with a break around the Indianapolis metropolitan area, where it merges with Interstate 465. It spans from Evansville, Indiana before it goes into Kentucky on the south side, and into the Michigan border just to the north of Angola, Indiana.

Route data was recorded by Purdue students during the summer of 2018, and it was identified that the section of I-69 between Crane and Bloomington, Indiana, which was recently finished in 2015, was a good section to experiment with Purdue NEXTCAR technologies [18]. Figure 2.2 is an image taken from Google Maps highlighting the start and end points used for testing on I-69. The northbound route was

used with latitude/longitude starting coordinates of 38.8632, -87.0703 and ending coordinates of 39.0709, -86.6125. Figure 2.3 shows vehicle velocity and grade for this section of I-69.

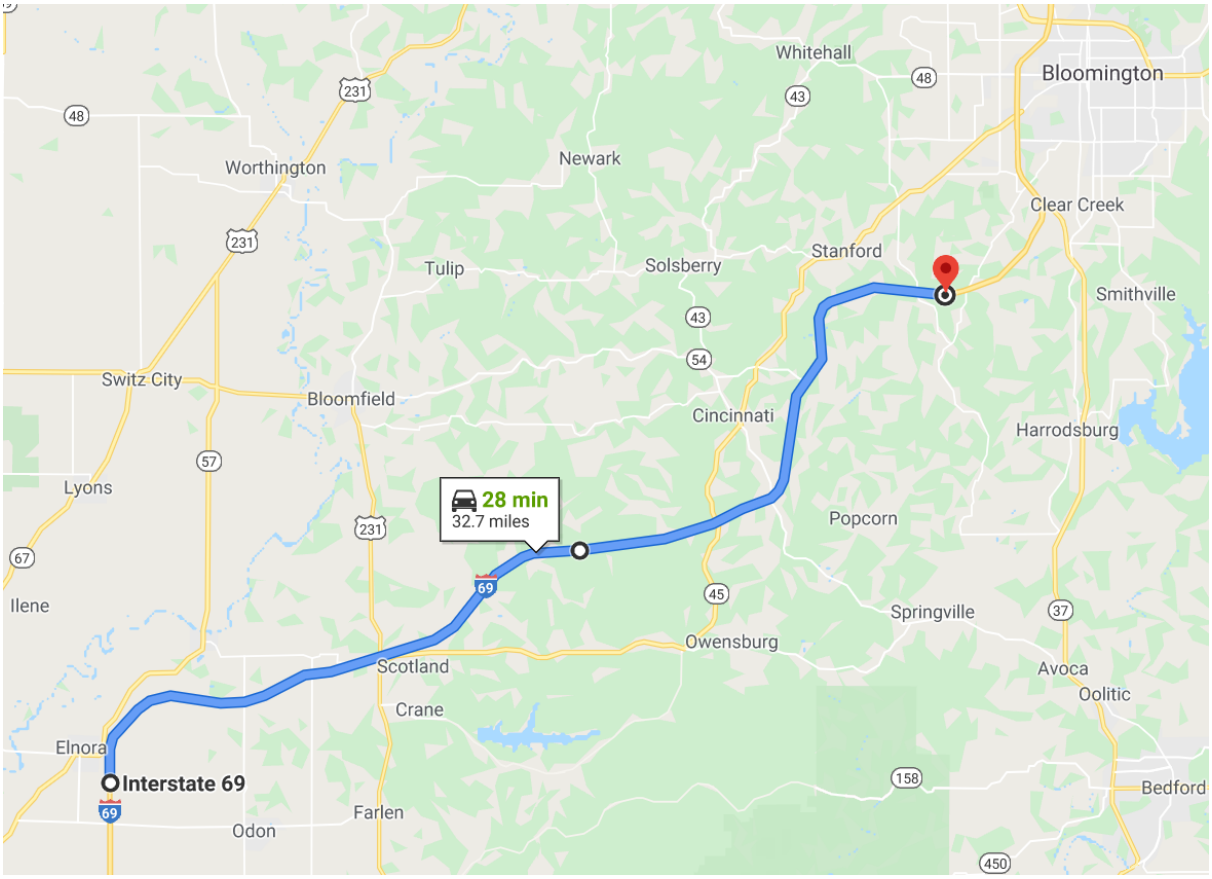

Fig. 2.2. Interstate 69

Figure 2.3's top plot shows a constant velocity vehicle traveling at the average traffic velocity over I-69 (27.5 m/s corresponds to approximately 61.5 MPH). The bottom plot shows the grade over time experienced by the same vehicle traveling at that velocity. Of note is that the grade has frequent oscillations and has amplitudes as high as nearly 5% and as low as nearly -5%.

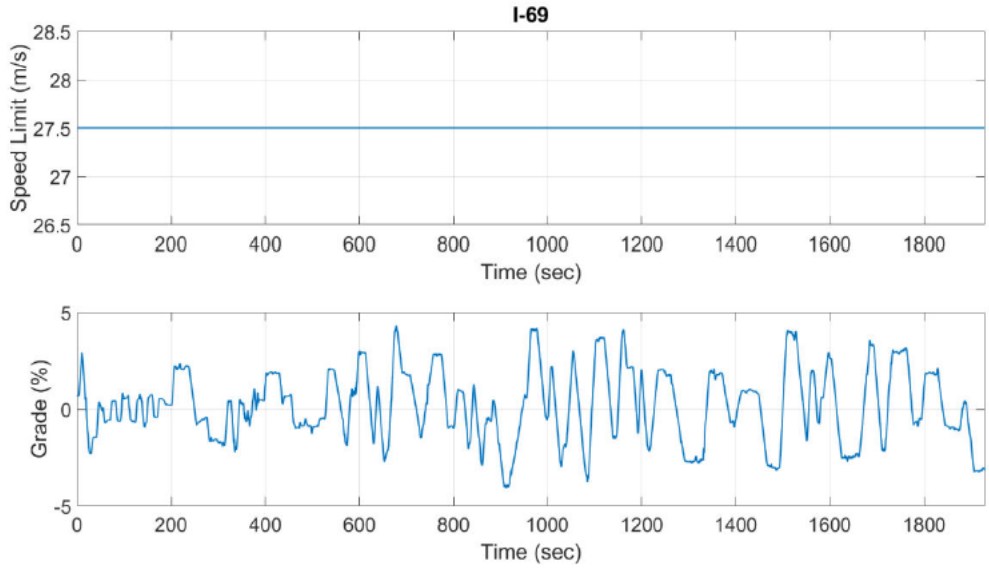

Fig. 2.3. Interstate 69 Speed and Grade Data

2.3.2 Interstate 280

Interstate 280 is also a north-south freeway that runs from San Jose to San Francisco in California. I-280 was identified by Peloton Technology as a route of interest for some of their on-road platooning testing. I-280 also has aggressive grade, and provides Peloton Technology with a close proximity route to test their technology and any updates or changes that they make to it. Road grade and average traffic speed data over this corridor was provided to Purdue by Peloton Technology. An image of Interstate 280 is shown in Figure 2.4; the data provided is for a roughly 30 mile section of the freeway.

The plots in Figure 2.5 show average traffic speed and road grade, in the same manner as Figure 2.3, for I-280. On the top, it can be seen that the traffic speed is given as 22.5 m/s which equates to approximately 50 MPH, and the bottom plot shows grade as a function of time for a vehicle following the constant velocity profile. The maximum and minimum grade values also reach nearly 5% and -5% respectively.

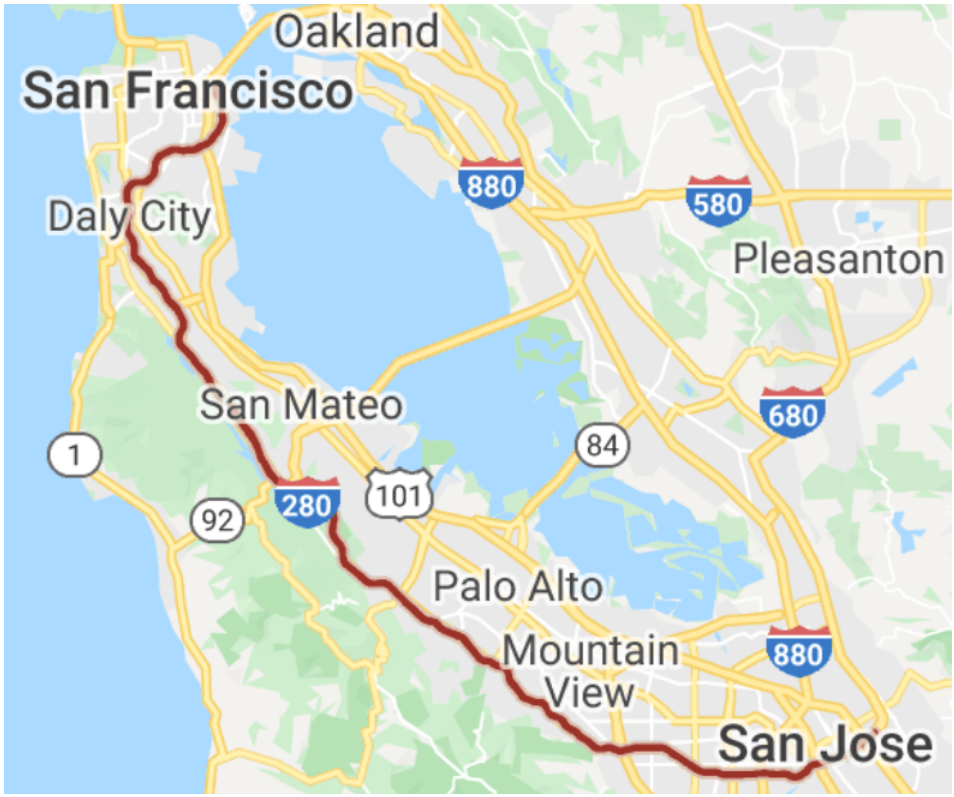

Fig. 2.4. Interstate 280

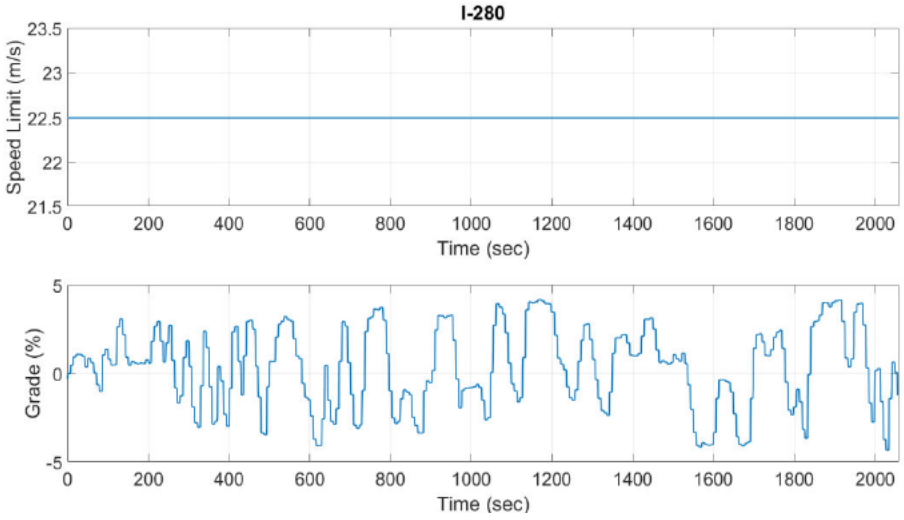

Fig. 2.5. Interstate 280 Speed and Grade Data

2.4 Test Cell vs. Simulation Fuel Consumption Initial Check

To both explore how test cell fuel consumption compares to simulation predicted fuel consumption, as well as work toward one of the NEXTCAR project goals of reducing fuel consumption by 5% using NEXTCAR developed algorithms (verified with the test cell), multiple tests were run on the testbed. Ultimately, the data of highest interest would come from the constant velocity vehicle baseline and the improved platooning lead and follow truck tests, because this yields the highest fuel savings percentage. However, in an attempt to identify how the test cell behaves with a variety of tests, single vehicle long-horizon predictive cruise control (LHPCC) and constant velocity platooning vehicles were also run. Table 2.1 shows both simulation and test cell fuel consumption numbers, as well as the fuel consumption percent differences between the test cell and simulation. The single vehicle and lead vehicle values are for a vehicle that was tracking a constant velocity. In the case of the follow vehicle, it was tracking a constant gap behind the lead vehicle. Table 2.2 gives the same information as 2.1, but substitutes the lead and single vehicle constant velocity profile with an optimized LHPCC velocity profile. The follow vehicle is then, of course, behind the LHPCC lead vehicle.

Table 2.1.
Constant Velocity Fuel Consumption Over I-280

	Single Vehicle	**Lead Vehicle**	**Follow Vehicle**
Simulation [lbs]	31.97	31.79	30.78
Test Cell [lbs]	30.71	30.57	27.52
Percent Difference [%]	-3.9	-3.8	-10.6

Each of the values in the test cell row represents a single data point (as each value comes from a single test), thus, drawing strong conclusions from this data was avoided (repeats of tests are covered in the following sections). Nonetheless, most tests

Table 2.2.
LHPCC Fuel Consumption Over I-280

	Single Vehicle	**Lead Vehicle**	**Follow Vehicle**
Simulation [lbs]	28.29	28.04	26.37
Test Cell [lbs]	27.45	27.22	25.72
Percent Difference [%]	-3.0	-2.9	-2.5

consistently consumed approximately 3% less fuel than their simulation counterparts. One major exception to this was the case of a follow vehicle tracking a fixed gap behind a lead vehicle tracking a constant velocity. It was initially speculated that there was an error with the testing equipment that yielded an erroneous value, so a second test was conducted for that data point. The second test yielded a fuel consumption of 27.73 lbs. This was .76% different than the initial test and -9.9% different from the simulation, which again, differed significantly more from simulation than the other tests did. It was hypothesized that this was due to differences in BSFC on the testbed versus in the vehicle model. However, due to time constraints and the fast paced nature of the NEXTCAR project, further investigation into the discrepancy was not conducted.

2.5 Fuel Savings of LHPCC and ROGG

After sanity checking the fuel consumption results from the test cell against simulation with the preliminary tests, the next step was to run multiple tests to obtain a statistically significant fuel savings percentage. The data in this section was used as part of the NEXTCAR project to fulfill a required milestone of a 5% fuel savings where the point of comparison was a single vehicle tracking a constant velocity. As part of closing out this milestone, two different strategies were used: 1) a two-truck platoon where the lead vehicle was using LHPCC and the follow vehicle was using

Peloton's production-intent PlatoonPro constant gap controller, and 2) a two-truck platoon where the lead vehicle was tracking a constant velocity and the follow vehicle was using a Purdue developed strategy called route optimized gap growth (ROGG). Data for both strategies was provided by Ifeoluwa Ibitayo [16]. Case #1 was given over I-280, and case #2 was given over I-69. The rationale for this was that these were the corridors where the respective strategies saved the most fuel in simulation (based on platoon average fuel consumption). After running the tests in section 2.4, it was discovered that the torque command output by the simulation framework was for dynamometer torque and not commanded engine torque. Because the X15 engine used in Purdue's Test Cell #2 has the accessories removed, an additional torque requirement to the dynamometer needed to be added to replicate the accessory loads. The data for the following sections will be based on the updated profiles with the added accessory loads.

2.5.1 Long Horizon Predictive Cruise Control + PlatoonPro Over I-280

A simulated constant velocity single-truck operating over the previously mentioned section of I-280 consumed, on average, 31.26 pounds of fuel in the test cell. This was the point of comparison from which the savings were measured. With the strategy of a LHPCC front truck with a constant gap PlatoonPro controlled rear truck, the average of the platoons' average fuel consumption was calculated to be 27.16 pounds. A t-test was then conducted, and the resulting calculation yielded a nominal savings of 13.11% with a confidence interval of $\pm 0.36\%$. This was for a confidence level of 95%.

Table 2.3 shows the amount of fuel consumed for each individual test. A total of 9 tests were run (3 tests to simulate each of the 3 different truck cases) in order to confirm fuel savings. Table 2.4 averages the fuel consumption of the lead and follow vehicles in order to visualize the platoon average savings.

Table 2.3.
Individual Engine Test Cell Fuel Consumption Over I-280

Test #	**Single Vehicle [lbs]**	**Lead Vehicle [lbs]**	**Follow Vehicle [lbs]**
1	31.24	28.13	26.32
2	31.27	27.92	26.25
3	31.26	28.09	26.24

Table 2.4.
Platoon Average Engine Test Cell Fuel Consumption Over I-280

Test #	**Single Vehicle [lbs]**	**Platoon Average [lbs]**
1	31.24	27.23
2	31.27	27.09
3	31.26	27.17
Average	31.26	27.16

2.5.2 Constant Velocity + Route Optimized Gap Growth Over I-69

The second strategy of a constant velocity lead vehicle with a follow vehicle using ROGG was simulated over I-69. The constant velocity single vehicle average fuel consumption over this corridor was 34.73 pounds, which was used as the point of comparison. The average of the platoons' average fuel consumption was 32.86 pounds. Another t-test was done, and the fuel savings were calculated to be 5.38% with a confidence interval of $\pm 0.22\%$. This was also for a confidence level of 95%. Fuel consumption numbers for all strategy 2 tests can be found in Table 2.5. Table 2.6 averages the lead and follow vehicles into a single column to more easily view the platoon average fuel savings.

Table 2.5.
Individual Engine Test Cell Fuel Consumption Over I-69

Test #	**Single Vehicle [lbs]**	**Lead Vehicle [lbs]**	**Follow Vehicle [lbs]**
1	34.69	34.51	31.18
2	34.76	34.45	31.33
3	34.75	34.49	31.19

Table 2.6.
Platoon Average Engine Test Cell Fuel Consumption Over I-69

Test #	**Single Vehicle [lbs]**	**Platoon Average [lbs]**
1	34.69	32.85
2	34.76	32.89
3	34.75	32.84
Average	34.73	32.86

2.6 Test Cell Repeatability Revisited

In addition to using the aforementioned tests to realize fuel savings using various strategies, they were also used as a check for the predicted fuel consumption values from simulation. This section explores the tests as a "real-world" reference to compare against the simulation values. Section 2.5 discussed the constant velocity single vehicle (used as a point of comparison), lead vehicle (in an improved platoon), and follow vehicle (in an improved platoon). Additionally, other tests were conducted in the spring of 2019 which included lead and follow vehicles in a standard (constant velocity) platoon. However, due to time constraints, the single vehicle LHPCC (non-platooning) vehicle was not retested. To reiterate, the following data represents tests that were run using the updated profiles with the accessory loads added.

2.6.1 Interstate 280

Table 2.7 shows values for a constant velocity single vehicle, a constant velocity platooning lead vehicle, and a follow vehicle tracking a constant gap using PlatoonPro behind the constant velocity lead vehicle. All of which are over the same section of I-280.

Table 2.7.
Test Cell vs. Simulation Fuel Consumption Constant Velocity Over I-280

Test Type	**Single [lbs]**	**Lead [lbs]**	**Follow [lbs]**
Constant Velocity Test Cell Test 1	31.24	31.13	30.16
Constant Velocity Test Cell Test 2	31.27	31.08	30.23
Constant Velocity Test Cell Test 3	31.26	31.09	30.14
Constant Velocity Test Cell Average	31.26	31.10	30.18
Constant Velocity Test Cell SD	0.0153	0.0265	0.0473
Constant Velocity Simulation	31.97	31.79	30.78
Percent Difference from Simulation	-2.22	-2.17	-1.95

Table 2.8 shows values for only a LHPCC lead vehicle with a PlatoonPro follow. It was determined that obtaining 3 tests for the LHPCC single vehicle profile with added accessory loads was the lowest priority in comparison to the other scenarios. This is why results for a LHPCC single vehicle are not included in Table 2.8

2.6.2 Interstate 69

Table 2.9 shows values for constant velocity single vehicle, constant velocity platooning lead, and follow vehicle using the ROGG strategy behind the constant velocity lead. Over the same section of I-69.

Table 2.8.
Test Cell vs. Simulation Fuel Consumption LHPCC Over I-280

Test Type	**Lead [lbs]**	**Follow [lbs]**
LHPCC Test Cell Test 1	28.13	26.32
LHPCC Test Cell Test 2	27.92	26.25
LHPCC Test Cell Test 3	28.09	26.24
LHPCC Test Cell Average	28.05	26.27
LHPCC Test Cell SD	0.1115	0.0436
LHPCC Simulation	28.04	26.37
Percent Difference from Simulation	0.04	-0.38

Table 2.9.
Test Cell vs. Simulation Fuel Consumption Constant Velocity Over I-69

	Single [lbs]	**Lead [lbs]**	**Follow [lbs]**
ROGG Test Cell Test 1	34.69	34.51	31.18
ROGG Test Cell Test 2	34.76	34.45	31.33
ROGG Test Cell Test 3	34.75	34.49	31.19
ROGG Test Cell Average	34.73	34.48	31.23
ROGG Test Cell SD	0.0379	0.0306	0.0839
ROGG Simulation	35.10	34.75	30.89
Percent Difference from Simulation	-1.05	-0.78	1.10

2.7 Summary

Two different NEXTCAR vehicle strategies, developed collaboratively by Purdue, Peloton Technology, and Cummins, have shown promising fuel savings over aggressively graded routes in the U.S. Long-horizon predictive cruise control on a lead truck

with a fixed gap platooning rear truck saved 13.11 ±0.36 % fuel over a section of I-280, and a constant velocity lead vehicle with a route optimized gap growth follow vehicle saved 5.38 ±0.22 % over a section of I-69. Furthermore, average test cell fuel consumption numbers deviated from simulation by 1.10% to -2.22%, and all testing datasets had standard deviation values less than 0.11 lbs of fuel, with the majority of tests having standard deviation values of less than 0.05 lbs of fuel. The strong correlation between test cell fuel consumption and simulation fuel consumption is a testament to the accuracy of the simulation framework.

3. TWO-TRUCK LONG-HORIZON PREDICTIVE CRUISE CONTROL

3.1 Motivation

When looking at fuel savings strategies to improve two-truck platooning, various improvements in vehicle dynamics have been explored. Investigated strategies include: optimizing lead vehicle velocity via a model predictive control (MPC) controller, optimizing follow vehicle gap via a MPC controller, the use of simultaneous shifting as a gap management strategy, and many others. However, what had not previously been investigated was a lead and follow vehicle simultaneously optimized to complete a corridor in a fixed amount of time. This, in theory, would provide the maximum fuel savings a two-truck platoon could achieve, as a solver is given complete control over both vehicles so long as it did not violate any physically based constraints (including engine power, braking power, and speed limits).

3.2 Two-Truck Long-Horizon Predictive Cruise Control Framework and Algorithm Design

In order to explore the optimal vehicle operation of a two-truck platoon, a linear model based on two Peterbilt 579 trucks was created for a MPC controller. This is referred to as two-truck long-horizon predictive cruise control (LHPCC). A state space representation was used, and the free body diagram, which was used for the state space equations, is shown in Figure 3.1.

The motive forces for the preceding and the follow truck were represented by the respective equations:

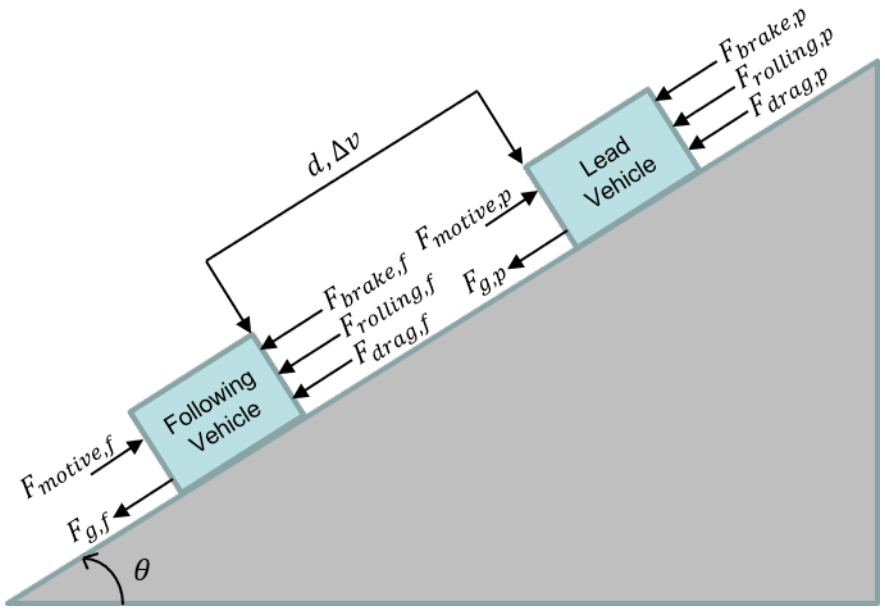

Fig. 3.1. Free-Body Diagram of Forces Acting on Two Class 8 Trucks

$$F_{motive,p} = P_{e,p}/V_p \tag{3.1}$$

$$F_{motive,f} = P_{e,f}/V_f \tag{3.2}$$

where $P_{e,p}$ is the engine power for the preceding vehicle, $P_{e,f}$ is the engine power for the follow vehicle, V_p is the preceding vehicle velocity, and V_f is the follow vehicle velocity. Power was used because it is independent of gear number which allows the nonlinearities associated with gear shifting to be neglected within the controller.

Similar equations were used to represent the braking forces:

$$F_{brake,p} = P_{brake,p}/V_p \tag{3.3}$$

$$F_{brake,f} = P_{brake,f}/V_f \tag{3.4}$$

where $P_{brake,p}$ and $P_{brake,f}$ are the preceding and follow vehicles' braking powers, respectively, and again V_p and V_f are the preceding and follow vehicles' velocities, respectively.

The force of gravity on the preceding and follow trucks, respectively, was represented by:

$$F_{gravity,p} = m_p g sin(\theta_p) \approx m_p g \theta_p \tag{3.5}$$

$$F_{gravity,f} = m_f g sin(\theta_f) \approx m_f g \theta_f \tag{3.6}$$

where m_p and m_f are the masses of the preceding and follow trucks, respectively, g is the acceleration due to gravity, θ_p is the grade experienced by the preceding truck, and θ_f is the grade experienced by the follow truck. The small angle approximation was used to approximate $sin(\theta_p)$ as θ_p and $sin(\theta_f)$ as θ_f.

The force of rolling resistance was represented by:

$$F_{roll,p} = m_p g f cos(\theta_p) \approx m_p g f \tag{3.7}$$

$$F_{roll,f} = m_f g f cos(\theta_f) \approx m_f g f \tag{3.8}$$

where m_p and m_f are the masses of the preceding and follow trucks, g is the acceleration due to gravity, and f is the rolling resistance coefficient. Again, the small angle approximation was used to approximate both $cos(\theta_f)$ and $cos(\theta_p)$ as 1.

The drag force varies as a function of both velocity and truck separation (which changes the drag coefficient). The drag forces were represented by:

$$F_{drag_p} = 1/2 \rho \bar{A} C_{D,0} (p_2 V_p \bar{V} + p_3 d \bar{V}^2) \tag{3.9}$$

$$F_{drag_f} = 1/2 \rho \bar{A} C_{D,0} (p_0 V_f \bar{V} + p_1 d \bar{V}^2) \tag{3.10}$$

where ρ is the density of air, $\bar{A}$ is the frontal area of the vehicle (assumed to be the same for both the preceding and follow vehicles because the model assumed identical vehicles in a platoon) $C_{D,0}$ is the nominal drag coefficient, which was assumed to be the same for both trucks since the model assumed identical preceding and follow vehicles, V_p is the current velocity of the preceding truck, V_f is the current velocity of the follow truck, $\bar{V}$ is the average velocity of the trucks (assuming negligible difference in their trip times), d is the distance between the preceding truck and the follow truck,

p_0 is the y-intercept of the linearization of drag as a function of distance for the follow truck, p_1 is the slope of the linearization of drag as a function of distance for the follow truck, p_2 is the y-intercept of the linearization of drag as a function of distance for the preceding truck, and p_3 is the slope of the linearization of drag as a function of distance for the preceding truck. This equation was obtained by linearizing the drag variation, a nonlinear phenomenon, as a function of truck separation. This data was obtained by Salari and is shown in Figure 3.2 [19]. A first-order Taylor expansion was then applied to the force of drag to obtain its variation as a linear function of both velocity and truck separation.

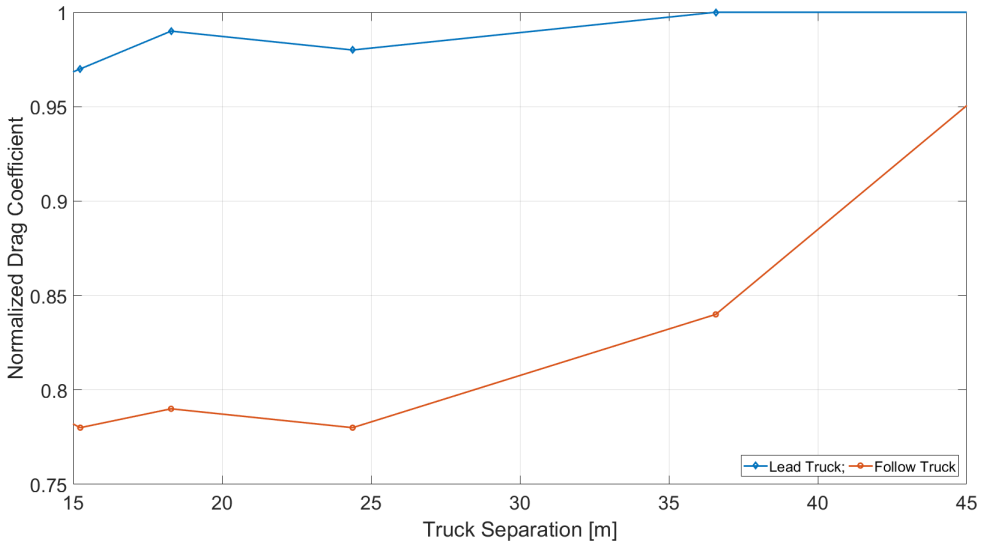

Fig. 3.2. The Normalized Drag Coefficients for the Lead Truck and Follow Truck as a Function of Truck Separation [19]

The prediction model for the system is as follows:

$$x[k+1] = \mathbf{A}x[k] + \mathbf{B}u[k] + \mathbf{B}_{\theta,\mathbf{f}}\theta_f[k] + \mathbf{B}_{\theta,\mathbf{p}}\theta_p[k] \tag{3.11}$$

where x is the state vector, $\mathbf{A}$ relates the evolution of states from one time instance to the next, u is the input vector, $\mathbf{B}$ relates how the inputs affect the states, θ_f is the road

grade experienced by the follow vehicle, $\mathbf{B}_{\theta,f}$ relates how the road grade experienced by the follow vehicle affects the states, θ_p is road grade experienced by the preceding vehicle, and $\mathbf{B}_{\theta,p}$ relates how the road grade experienced by the preceding vehicle affects the states. The road grade experienced by the preceding vehicle and follow vehicle were treated as disturbances so that they could change dynamically over the MPC horizon.

The state vector is as follows:

$$x = \begin{bmatrix} S_f \\ V_f \\ P_{e,f} \\ P_{b,f} \\ f \\ d \\ S_p \\ V_p \\ P_{e,p} \\ P_{b,p} \end{bmatrix} \tag{3.12}$$

where S_f is the position of the follow vehicle. V_f is the velocity of the follow vehicle. $P_{e,f}$ is the engine power of the follow vehicle. $P_{b,f}$ is the braking power of the follow vehicle. f is the rolling resistance coefficient. d is the distance between the preceding vehicle and the follow vehicle. S_p is the position of the preceding vehicle. V_p is the velocity of the preceding vehicle. $P_{e,p}$ is the engine power of the preceding vehicle. $P_{b,p}$ is the braking power of the preceding vehicle.

The state matrix, $\mathbf{A}$, is as follows:

$$\mathbf{A} = \begin{bmatrix} 0 & 1 & 0 & 0 & 0 & 0 & 0 & 0 & 0 & 0 \\ 0 & -\frac{\rho \bar{A} C_{D,0} \bar{V} p_0}{2m_{e,f}} & \frac{\eta_t}{m_{e,f}\bar{V}} & -\frac{1}{m_{e,f}\bar{V}} & -\frac{m_f}{m_{e,f}}g & -\frac{\rho \bar{A} C_{D,0} \bar{V}^2 p_1}{2m_{e,f}} & 0 & 0 & 0 & 0 \\ 0 & 0 & -\frac{1}{\tau_e} & 0 & 0 & 0 & 0 & 0 & 0 & 0 \\ 0 & 0 & 0 & -\frac{1}{\tau_b} & 0 & 0 & 0 & 0 & 0 & 0 \\ 0 & 0 & 0 & 0 & 0 & 0 & 0 & 0 & 0 & 0 \\ 0 & -1 & 0 & 0 & 0 & 0 & 0 & 1 & 0 & 0 \\ 0 & 0 & 0 & 0 & 0 & 0 & 0 & 1 & 0 & 0 \\ 0 & 0 & 0 & 0 & -\frac{m_p}{m_{e,p}}g & -\frac{\rho \bar{A} C_{D,0} \bar{V}^2 p_3}{2m_{e,p}} & 0 & -\frac{\rho \bar{A} C_{D,0} \bar{V} p_2}{2m_{e,p}} & \frac{\eta_t}{m_{e,p}\bar{V}} & -\frac{1}{m_{e,p}\bar{V}} \\ 0 & 0 & 0 & 0 & 0 & 0 & 0 & 0 & -\frac{1}{\tau_e} & 0 \\ 0 & 0 & 0 & 0 & 0 & 0 & 0 & 0 & 0 & -\frac{1}{\tau_b} \end{bmatrix} \tag{3.13}$$

where ρ is the density of air. $\bar{A}$ is the frontal area of the vehicle, which was assumed to be the same for both the preceding and follow vehicles because the model assumed identical vehicles in a platoon. $C_{D,0}$ is the nominal drag coefficient, which is again the same for both vehicles as previously mentioned. $\bar{V}$ is the average velocity of the vehicles over the route (again, assumed to be the same for both vehicles). p_0 is the y-intercept of the linearization of drag as a function of distance for the follow vehicle. p_1 is the slope of the linearization of drag as a function of distance for the follow vehicle. p_2 is the y-intercept of the linearization of drag as a function of distance for the preceding vehicle. p_3 is the slope of the linearization of drag as a function of distance for the preceding vehicle. $m_{e,f}$ is the inertial mass of the follow vehicle. $m_{e,p}$ is the inertial mass of the preceding vehicle. η_t is the vehicle drivetrain efficiency which is assumed to be the same for both vehicles. m_f is the mass of the follow vehicle. m_p is the mass of the preceding vehicle. g is the acceleration due to gravity. τ_e is the engine time constant, and τ_b is the brake time constant; both of which were assumed to be the same for both vehicles due to the assumption of identical powertrains and braking systems.

The input vector is as follows:

$$u = \begin{bmatrix} P_{e,f,com} \\ P_{brake,f,com} \\ P_{e,p,com} \\ P_{brake,p,com} \end{bmatrix} \tag{3.14}$$

where $P_{e,f,com}$ is the commanded engine (positive) power of the follow vehicle, $P_{b,f,com}$ is the commanded braking (negative) power of the follow vehicle, $P_{e,p,com}$ is the commanded engine (positive) power of the preceding vehicle, $P_{b,p,com}$ is the commanded braking (negative) power of the preceding vehicle.

The input matrix, $\mathbf{B}$, is as follows:

$$\mathbf{B} = \begin{bmatrix} 0 & 0 & 0 & 0 \\ 0 & 0 & 0 & 0 \\ \frac{1}{\tau_e} & 0 & 0 & 0 \\ 0 & \frac{1}{\tau_b} & 0 & 0 \\ 0 & 0 & 0 & 0 \\ 0 & 0 & 0 & 0 \\ 0 & 0 & 0 & 0 \\ 0 & 0 & 0 & 0 \\ 0 & 0 & \frac{1}{\tau_e} & 0 \\ 0 & 0 & 0 & \frac{1}{\tau_b} \end{bmatrix} \tag{3.15}$$

where τ_e is the engine time constant, and τ_b is the brake time constant. Both of which are assumed to be the same for the preceding and follow vehicles as previously mentioned.

The grade input matrix for the follow vehicle, $\mathbf{B}_{\theta,f}$, is as follows:

$$\mathbf{B}_{\theta,\mathbf{f}} = \begin{bmatrix} 0 \\ -\frac{m_f}{m_{e,f}}g \\ 0 \\ 0 \\ 0 \\ 0 \\ 0 \\ 0 \\ 0 \\ 0 \end{bmatrix} \tag{3.16}$$

where m_f and $m_{e,f}$ are the mass and inertial mass, respectively, of the follow vehicle, and g is the acceleration due to gravity.

The grade input matrix for the preceding vehicle, $\mathbf{B}_{\theta,p}$, is as follows:

$$\mathbf{B}_{\theta,\mathbf{p}} = \begin{bmatrix} 0 \\ 0 \\ 0 \\ 0 \\ 0 \\ 0 \\ 0 \\ -\frac{m,p}{m_{e,p}}g \\ 0 \\ 0 \end{bmatrix} \tag{3.17}$$

where m_p and $m_{e,p}$ are the mass and inertial mass, respectively, of the preceding vehicle, and g is the acceleration due to gravity.

The objective function is as follows:

$$min\ J = \sum_{k=0}^{N-1} P_{e,p}[k] + P_{e,f}[k] \tag{3.18}$$

$$\tag{3.19}$$

the constraints for the two-truck MPC are shown below:

$$P_{e,min} \leq P_{e,p} \leq P_{e,max} \tag{3.20}$$

$$P_{e,min} \leq P_{e,f} \leq P_{e,max} \tag{3.21}$$

$$\dot{P}_{e,min} \leq \dot{P}_{e,p} \leq \dot{P}_{e,max} \tag{3.22}$$

$$\dot{P}_{e,min} \leq \dot{P}_{e,f} \leq \dot{P}_{e,max} \tag{3.23}$$

$$\ddot{P}_{e,min} \leq \ddot{P}_{e,p} \leq \ddot{P}_{e,max} \tag{3.24}$$

$$\ddot{P}_{e,min} \leq \ddot{P}_{e,f} \leq \ddot{P}_{e,max} \tag{3.25}$$

$$0 \leq P_{brake,p} \leq P_{brake,max} \tag{3.26}$$

$$0 \leq P_{brake,f} \leq P_{brake,max} \tag{3.27}$$

$$V_{min} \leq V_p \leq V_{max} \tag{3.28}$$

$$V_{min} \leq V_f \leq V_{max} \tag{3.29}$$

$$d_{min} \leq d \leq d_{max} \tag{3.30}$$

$$t_{final} \leq t_{max} \tag{3.31}$$

where $P_{e,p}$ and $P_{e,f}$ are the respective preceding and follow vehicles' engine powers. $P_{e,min}$ is the minimum engine power (i.e., maximum retarder power), and $P_{e,max}$ is the maximum positive engine, both of which were assumed to be the same for both vehicles. $\dot{P}_{e,p}$ and $\dot{P}_{e,f}$ are the rates of change of engine power for the preceding and follow vehicles, respectively. $\dot{P}_{e,min}$ is the fastest that the engine power can decrease, and $\dot{P}_{e,max}$ is the fastest that the engine power can increase, both of which were assumed to be the same for both vehicles. $\ddot{P}_{e,p}$ and $\ddot{P}_{e,f}$ are the second derivatives of engine power for the preceding and follow vehicles, respectively. $\ddot{P}_{e,min}$ is the fastest that the derivative of engine power can decrease, and $\ddot{P}_{e,max}$ is the fastest that the

derivative of engine power can increase, both of which were assumed to be the same for both vehicles. $P_{brake,p}$ and $P_{brake,f}$ are the braking powers of the preceding and follow vehicles, respectively. $P_{b,max}$ is the maximum braking power, which was assumed to be the same for both vehicles. d is the instantaneous vehicle separation, d_{min} is the minimum platooning gap, and d_{max} is the maximum platooning gap. t_{final} is the final time instance, and t_{max} is the maximum time allowed to finish the corridor.

Essentially, the objective is to minimize positive power (used as a proxy for fuel consumption) of both the preceding and follow vehicles while maintaining realistic constraints on the engines, brakes, vehicle separation and also ensuring that the vehicles finish the route within the specified time constraint. The controller was applied to the entire route in open loop to generate an optimal preceding vehicle velocity $V_{p,des}$, and an optimal vehicle separation (gap), d_{des}, for the follow vehicle to platoon at.

3.3 Results

3.3.1 I-69 and I-280 Results

After finishing the algorithm development, the model was exercised over the sections of I-69 and I-280 that were outlined in chapter 2. An interesting, and somewhat non-intuitive, result is that the algorithm nearly always output a near fixed gap desired gap profile with the setpoint being the smallest gap allowed by the gap constraints. This can be seen for the I-280 corridor in Figure 3.3, and in Figure 3.4 for the I-69 corridor.

In Figures 3.3 and 3.4, it can be seen that there are five instances of small desired gap growth over the I-280 corridor, and two very small (effectively negligible) instances of desired gap growth over the I-69 corridor. This implies that over the two corridors outlined in this thesis, fixed gap platooning behind a lead truck with an optimized velocity profile appears to be the most optimal way to operate two vehicles (especially in the case over I-69).

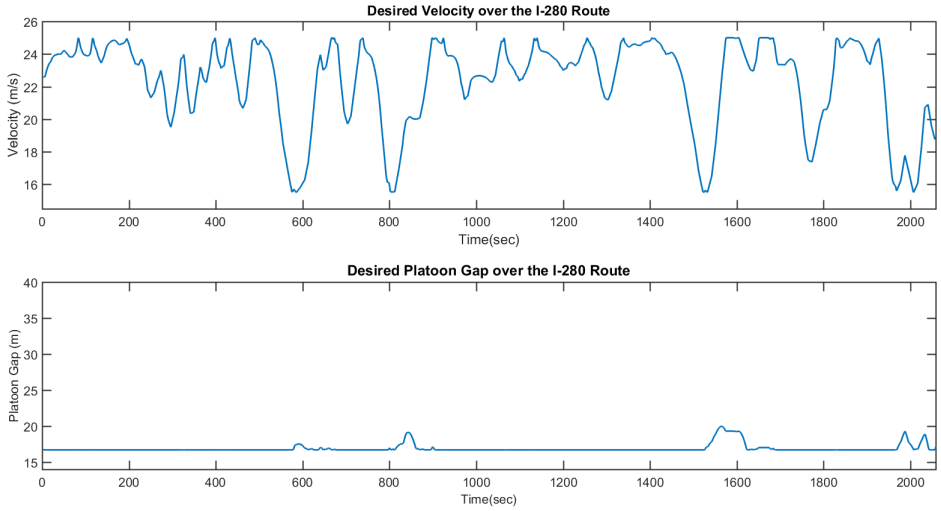

Fig. 3.3. Interstate 280 Optimized Velocity & Gap

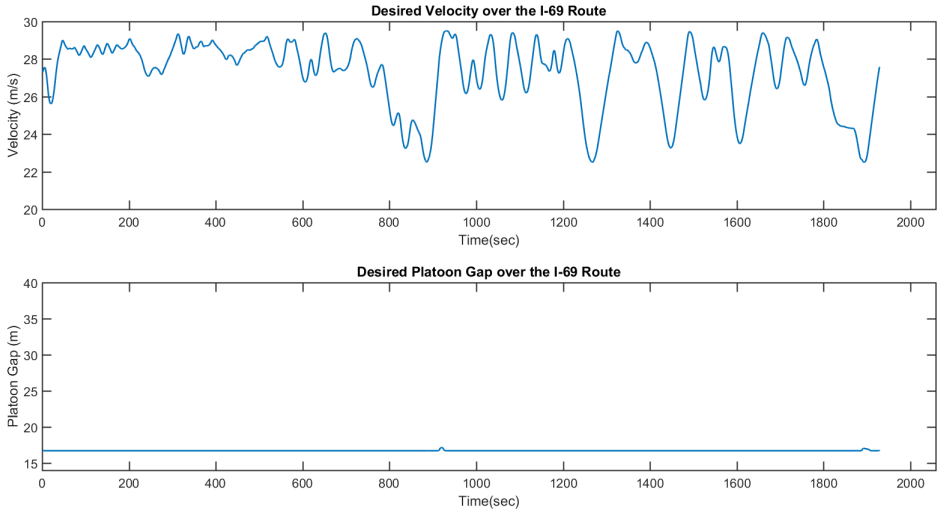

Fig. 3.4. Interstate 69 Optimized Velocity & Gap

3.3.2 Further Exploration over I-69

Because this was a Purdue-led effort with plans for on-road testing (over I-69), further exploration of the model was done using the I-69 corridor. This was done to

test some of the limits of the model and allow for further insight into what optimal two-truck behavior looks like.

The discovery of fixed gap platooning behind an optimized lead truck was further tested by first adjusting the minimum constraint on platoon gap over I-69. This is shown in Figure 3.5

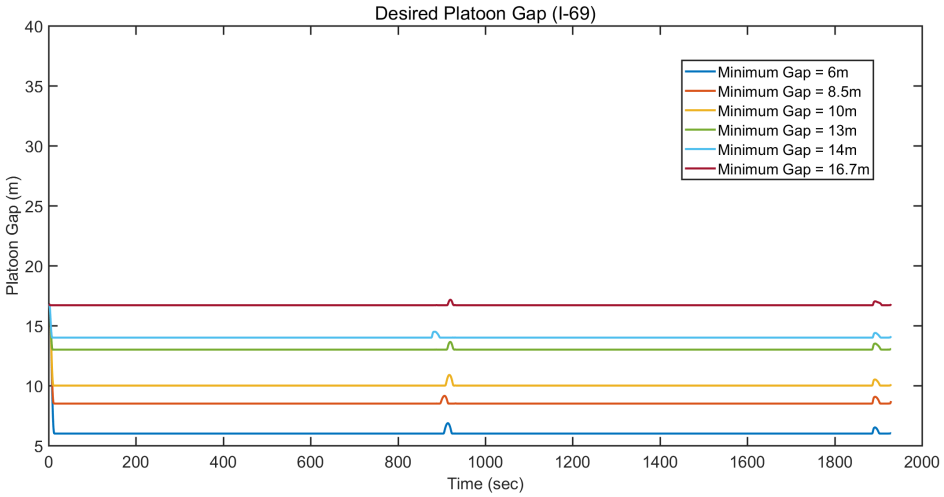

Fig. 3.5. Interstate 69 Optimized Gap with Different Minimum Gap Constraints

Figure 3.5 shows that even when the minimum platooning gap was changed, the optimal gap profile of the follow vehicle was still a fixed gap at the minimum allowable gap. In all six different minimum gap constraint scenarios, it can be seen that the two (near negligible) gap growths still occurred at roughly the same instances over the route. This outcome indicates that, if the lead truck is driven very reasonably (and with knowledge of a follow truck behind it), a follow vehicle should be able to easily track a fixed gap without needing to aggressively speed up or slow down.

Given the outcome of the previous results, the next exercise was to adjust the mass of the trucks. Intuitively, as the mass of a truck becomes larger, the fixed maximum forces (from the engine and the brakes) will have less of an effect on its change in acceleration. This would, in theory, make it more difficult to follow a fixed gap (especially in the case of a heavier rear truck). The outcome of these tests are

shown in Figure 3.6. Four cases are shown: (1) standard front truck with light rear truck, (2) light front truck with standard rear truck, (3) standard front truck with heavy rear truck, and (4) heavy front truck with standard rear truck.

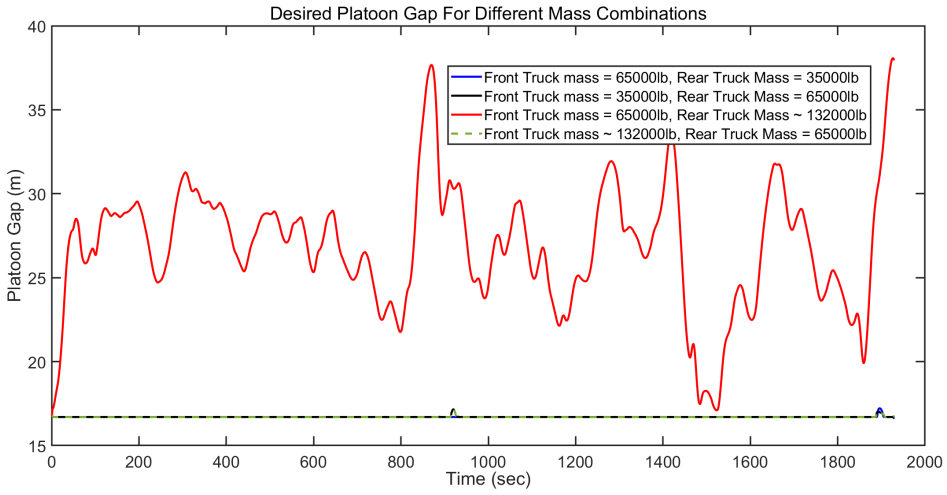

Fig. 3.6. Interstate 69 Optimized Gap for Different Truck Masses

Again in Figure 3.6, it can be seen that fixed gap platooning was the optimal strategy when the lead truck had an optimized velocity profile. Even in case two where the rear truck was nearly twice the mass of the lead truck, a fixed gap platoon was still optimal. The only deviation from this was when the rear truck mass was doubled, and in this scenario there is significant change in gap. However, it is important to highlight that this was an academic exercise. The maximum GVW of a tractor-trailer is 80,000 pounds. This means that the tested value of 132,000 pounds is well beyond the legal limit; indicating that for all practical purposes, weight does not affect the optimal gap profile over I-69. Additionally, even though the second case (with a heavier rear truck) also output fixed gap platooning, it should be noted that, currently, Peloton's PlatoonPro system allows for platooning with only the heavier truck in front, for safety reasons.

3.3.3 Fuel Consumption

Once the two-truck MPC model had been further investigated, and subsection 3.3.2 has shown that fixed gap platooning did really appear to be the optimal strategy behind a well-driven lead vehicle, a look into simulated fuel savings was appropriate. Because the results indicate that a fixed minimum gap is most optimal, it was helpful to compare the two-truck LHPCC results to a "selfish" single-truck optimized LHPCC. Both strategies were given a rear truck using fixed gap PlatoonPro (both with and without simultaneous shifting). The results for I-280 are shown in Table 3.1, and they show fuel savings of ∼14% with respect to a single vehicle tracking a constant velocity (which consumed 14.51 kg of fuel). The results for I-69 are shown in Table 3.2, and they demonstrate fuel savings of ∼12% with respect to a single vehicle tracking a constant velocity (which consumed 15.92 kg of fuel).

Table 3.1.
Interstate 280 Fuel Consumption Results

Strategy over I-280			Cumulative Positive Energy (MJ)		% Reduction (With Respect to Baseline)		Fuel Consumption (kg) & % Savings (Baseline: 14.51 kg)		Braking Energy (MJ) (Baseline: 48.64 MJ)		Estimated Potential Fuel Savings (kg)
Two Truck Platoon (Without Simultaneous Shifting)	LHPCC (via MPC) + PP	Front Truck	223.36	219.00	14.26%	15.94%	12.76	12.51 (13.78%)	13.62	17.4	0.99 (20.6%)
		Rear Truck	214.63		17.61%		12.25		21.21		
	Two Truck MPC + PP	Front Truck	226.81	221.22	12.94%	15.09%	12.89	12.60 (13.16%)	17.36	19.9	1.13 (21.0%)
		Rear Truck	215.62		17.23%		12.30		22.45		
Two Truck Platoon (With Simultaneous Shifting)	LHPCC (via MPC) + PP	Front Truck	223.25	217.08	14.31%	16.68%	12.75	12.42 (14.40%)	13.62	16.2	0.93 (20.8%)
		Rear Truck	210.91		19.04%		12.08		18.85		
	Two Truck MPC + PP	Front Truck	226.70	219.36	12.98%	15.80%	12.89	12.51 (13.78%)	17.36	18.7	1.07 (21.2%)
		Rear Truck	212.01		18.62%		12.13		20.03		

Table 3.1 (for I-280) shows that slightly higher fuel savings were achieved with the "selfish" single-truck velocity profile than with the two-truck front vehicle velocity profile. It is speculated that this could have partially been due to the fact that the optimized I-280 rear truck gap profile did not spend as much time against the mini-

Table 3.2.
Interstate 69 Fuel Consumption Results

Strategy over I-69			Cumulative Positive Energy (MJ)		% Reduction (With Respect to Baseline)		Fuel Consumption (kg) & % Savings (Baseline: 15.92 kg)		Braking Energy (MJ) (Baseline: 24.82 MJ)		Estimated Potential Fuel Savings (kg)
Two Truck Platoon (Without Simultaneous Shifting)	LHPCC (via MPC) + PP	Front Truck	266.79	254.52	8.72%	12.92%	14.69	14.06 (11.68%)	0.94	3.2	0.18 (12.8%)
		Rear Truck	242.25		17.12%		13.43		5.46		
	Two Truck MPC + PP	Front Truck	268	254.25	8.31%	13.01%	14.65	13.98 (12.15%)	1.34	2.2	0.12 (12.9%)
		Rear Truck	240.5		17.71%		13.32		3.01		
Two Truck Platoon (With Simultaneous Shifting)	LHPCC (via MPC) + PP	Front Truck	266.66	253.96	8.77%	13.11%	14.68	14.02 (11.93%)	0.93	2.8	0.15 (12.9%)
		Rear Truck	241.26		17.46%		13.36		4.63		
	Two Truck MPC + PP	Front Truck	267.95	253.85	8.33%	13.15%	14.65	13.96 (12.31%)	1.34	2.0	0.11 (13.0%)
		Rear Truck	239.75		17.98%		13.27		2.6		

mum gap constraint as in the case of I-69 (per Figure 3.3 above), and this desired gap growth did not occur in the vehicle simulation framework when fixed gap PlatoonPro was used. Another likely explanation is that the linear model did not capture all of the nuanced truck behaviors that the high-fidelity model did (e.g., shifting). Nonetheless, Figure 3.7 shows how the lead truck velocity profiles were similar between the two-truck optimized MPC and single-truck optimized MPC.

Lastly, further analysis of the data shown in Tables 3.1 and 3.2 was conducted to investigate what could potentially be done to realize more fuel savings. In order to do this, a series of calculations were done. First, the amount of fuel consumed over the corridor was divided by the cumulative propulsive energy. This provided an estimate for how much fuel it took to put a given amount of energy into the vehicle (an efficiency of sorts). This number can then be multiplied by the cumulative amount of negative energy, used by the retarder, to arrive at an estimate of how much additional fuel could be saved if no retarder were to be used over the corridor. These results are shown on the rightmost column in both Tables 3.1 and 3.2. The respective percent savings from the baseline, if the calculated amount of fuel savings from retarder

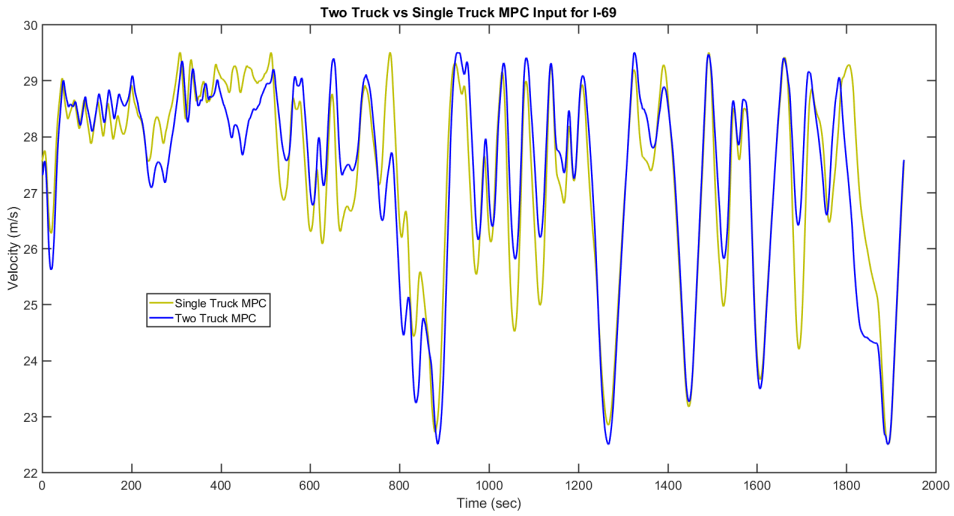

Fig. 3.7. Interstate 69 Optimized Velocity Comparison

elimination were to be realized, are also shown in parentheses in the same column. From this, it can be deduced that if the retarder were to be completely eliminated over the I-280 corridor, savings of roughly 20% could be realized. This is due to the fact that the vehicles use more retarder (cumulative braking energy) over I-280 than over I-69; therefore, there is more potential fuel savings to be had over I-280. However, in order to completely eliminate the retarder usage (and therefore realize more fuel savings), the velocity constraints would need to allow a wider range. Because the MPC controller uses a linear model to solve for the optimal velocity and gap profiles, but the force due to drag is quadratic (not linear), when the velocity constraints are more flexible than outlined in this chapter, the model's predictive ability of what is optimal becomes less accurate. When the, further relaxed, "optimized" velocity profile is fed into the high-fidelity vehicle model, more fuel is consumed at the higher velocities than the solver anticipated, and therefore overall savings are not improved. Thus, in order to realize more savings over I-280, the drag term would need to be modeled differently.

3.4 Summary

The conclusion that can be drawn up to this point in the two-truck MPC development is that when a lead truck has its velocity profile optimized, the rear truck is able to efficiently maintain the minimum allowable gap. Maintaining the minimum possible platoon gap allows both trucks to reap the maximum benefit of platooning and reduce the energy lost to drag as much as possible. When this was done, fuel savings were ∼14% and ∼12% over I-280 and I-69, respectively. Further analysis of the retarder energy indicated that if the retarder could be completely eliminated, fuel savings of ∼20% and ∼13% over I-280 and I-69, respectively, could potentially be realized. The serendipitous aspect of this is that no further development of a variable gap platoon controller would need to be developed; Peloton's PlatoonPro controller already tracks a constant gap.

4. TWO-TRUCK FUEL SAVINGS

4.1 Motivation

After extensive research and development of candidate algorithms for optimal vehicle dynamics from months of testing in both the simulation space as well as the engine test cell, the appropriate next step was to conduct on-road testing. Because this testing would be Purdue-led, the focus remained exclusively on a roughly 40 mile section of Interstate 69, which is approximately a 2 hour one-way drive from the Purdue truck facility in Lafayette, IN.

Due to the novel SARS-CoV-2 virus, platooning of two trucks was unavailable. Therefore, real-world single-truck data was collected to be run in platooning simulations. When deemed safe and appropriate, real-world fuel economy testing (J1321 Type II) over I-69 is planned, in order to have on-highway results of realized fuel savings.

Having experimental data from on-road trucks to run in simulation has a number of benefits. First, it allows for the characterization of the cruise controller, which is a better representation of baseline truck behavior, from which fuel savings can be measured. Second, it allows for the validation of on-truck variable velocity (LHPCC) control, ensuring that the on-road truck can track desired velocity profiles. Lastly, it also allows for fuel consumption predictions that are one step closer to what could be expected from on-road vehicles; the simulated fuel consumption would come from velocity profiles that were experimentally obtained.

4.2 Experimental Setup and Testing Procedure

For on-road testing, two 2019 Peterbilt 579 sleeper cabs were used. They are powered by the Cummins X15 Efficiency Series engine (same engine in Purdue's Herrick Labs test cell #2) mated to an Eaton Endurant 12 speed automated manual transmission. The trucks are connected to 53' Wabash National DuraPlate dry van trailers with trailer skirts, and they are loaded down with concrete blocks so that the total tractor-trailer GVW is 65,000 lbs. The vehicles are shown in Figure 4.1.

Fig. 4.1. Peterbilt 579 Trucks

The trucks are equipped with Peloton's PlatoonPro system, which is integrated into the vehicle's controller area network (CAN). This allows the PlatoonPro system to read data from the vehicle, engine, transmission, and brake module. It also allows for various parameters, such as engine torque, to be commanded during a platoon. The data obtained in this section comes from Peloton's engine control unit (PECU), which has an internal GPS that allows it to log vehicle parameters as a function of time and location.

Speedgoat real-time target machines were installed to enable the implementation of custom Simulink algorithms. The Speedgoat machines are equipped with separate GPS units, and they are able to communicate both over CAN and through separate connections to the engine and PECU. This gives them the ability to command engine

torque, retarder torque, transmission gear number, and cruise control setpoint. In this chapter, only the use of variable cruise control setpoint was used to command a variable velocity LHPCC Profile. The network architecture is shown in Figure 4.2.

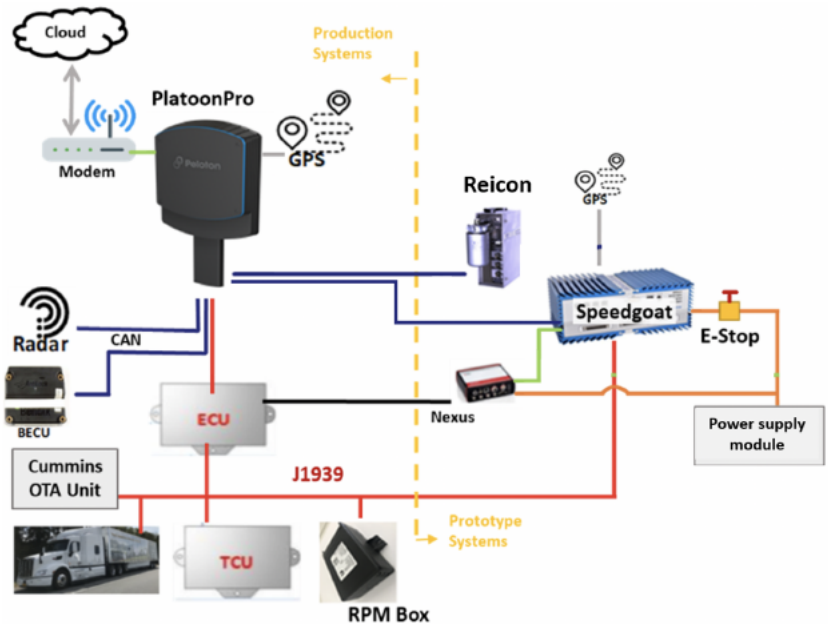

Fig. 4.2. Truck Vehicle Network Schematic

In the spirit of trying to mimic J1321 Type II fuel testing procedures, even though no official on-road fuel economy testing was conducted, the vehicle was driven down to the testing location, outlined in section 4.3, immediately before testing. This allowed for the vehicle's hardware to reach operating temperature, which helped ensure the vehicle was in the same state for each test.

4.3 Interstate 69 Corridor

Upon further analysis of the portion of I-69 that was used for the research outlined in chapters 2 and 3, the current section that was used could be improved, from the perspective of truck testing, by giving the starting and ending points identifiable landmarks, as well as placing them in locations such that if a test needed to be aborted, the time to regroup and reset is minimized. The landmark identification is

useful in ensuring the test equipment is performing as expected in the instance that it is supposed to initiate a test sequence.

The southern, starting, point was moved around half a mile north to be on a bridge spanning railroad tracks, and the northern, ending, point was also moved about 5 miles north to be at the South Rockport Road underpass that is between the Fullerton Pike exit and the Highway 37 exit. This provided a quick turnaround in the case of an improper start for the first, beginning of the day, southbound test. While this thesis focuses on the northbound testing, a southbound test preceded every northbound test due to proximity from Purdue's campus. The previous northern point would have led to a roughly 20 minute reset time versus approximately 5 minutes that it took in the new route. The new starting GPS coordinates were 38.868301, -87.070196, and the new ending GPS coordinates were 39.118228, -86.567221. The updated route is shown in Figure 4.3.

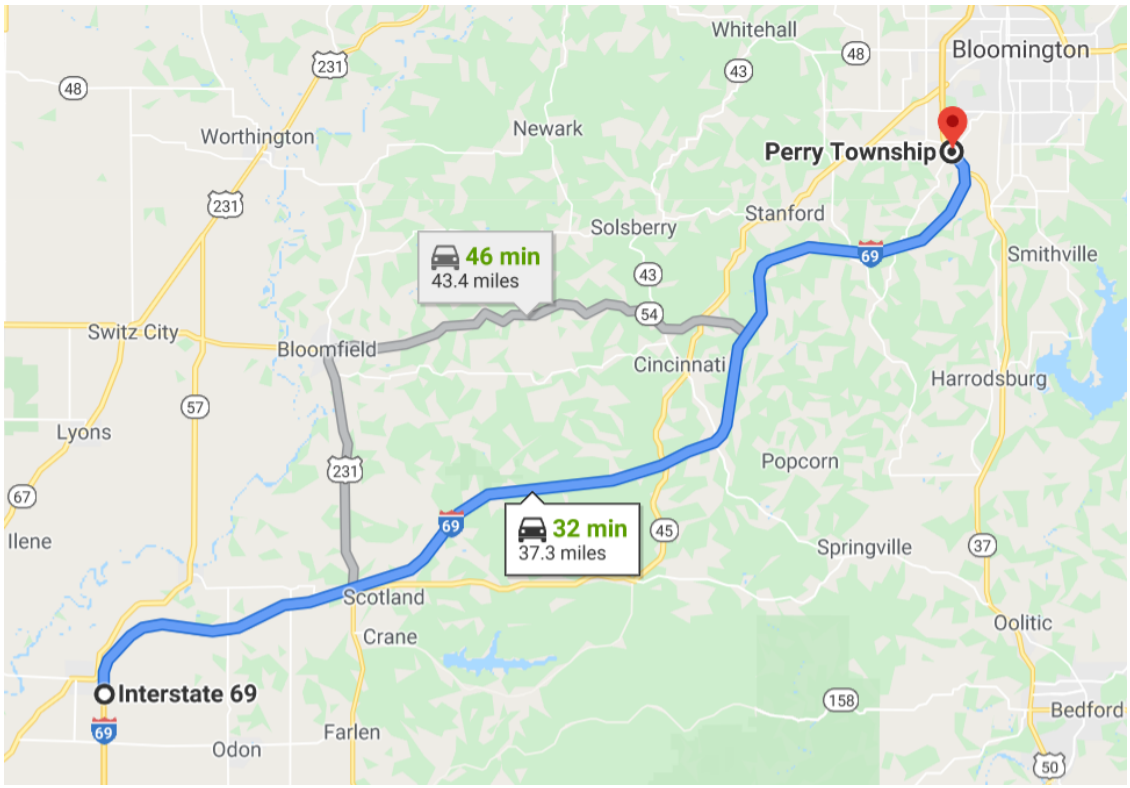

Fig. 4.3. Updated I-69 Route

A zoomed in view of the change made to the start point (southern location) is shown in Figure 4.4, and a zoomed in view of the change made to the end point (northern location) is shown in Figure 4.5. In both cases, the original location is the circle with the black outline, and the new location is the red pin.

Fig. 4.4. Updated I-69 Route Starting Point

A standard day of testing started with the drive down to I-69 from Lafayette. A stop was then made on the southbound ramp onto I-69 from Fullerton Pike to ensure all equipment and software were prepared for testing. A southbound test was then run to the aforementioned southbound point on I-69. Finally, the truck then took the US Highway 58 exit to pause briefly for another system functionality check before beginning the northbound testing, which began as soon as the GPS in the truck recorded the vehicle crossing the starting point.

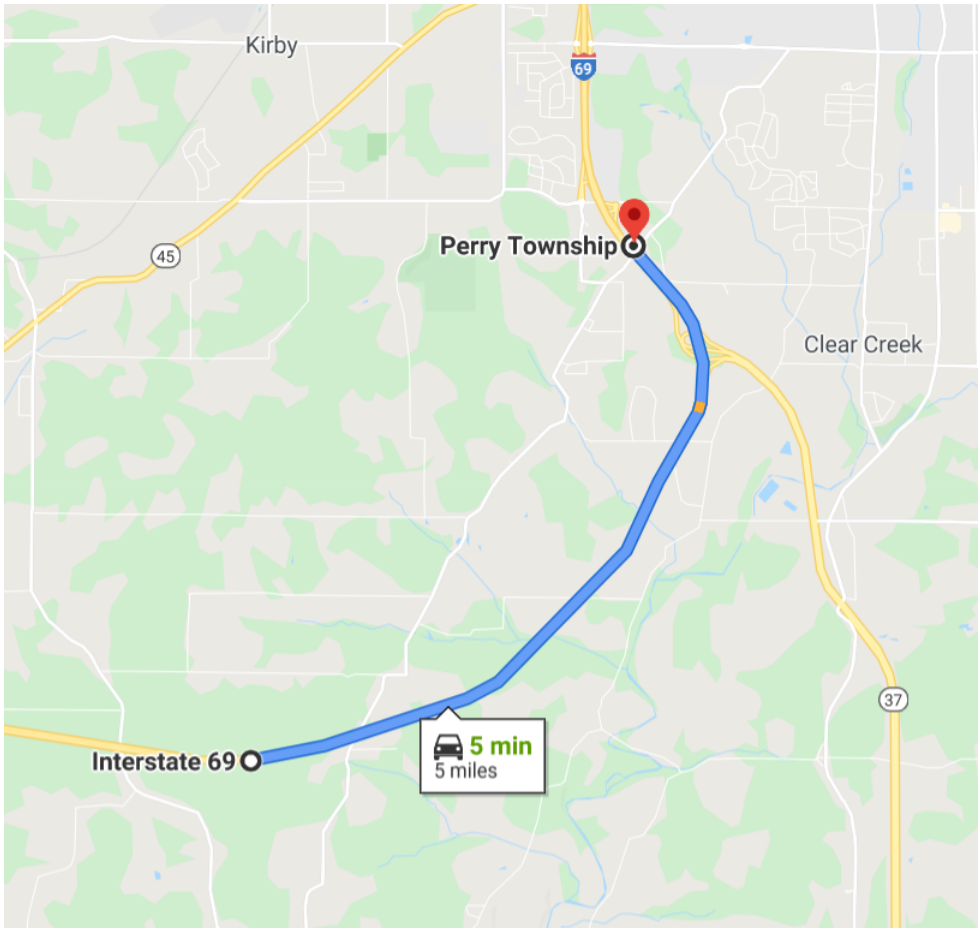

Fig. 4.5. Updated I-69 Route Ending Point

It should be noted that tests on both the northbound and southbound routes were conducted, but this thesis will focus exclusively on the northbound route. The primary rationale for this is that previous research conducted by Professor Greg Shaver et al. concentrated exclusively on the northbound route. For sake of continuity of the progression of work that has been done up until this point in time (Summer 2020), only results for the northbound route will be discussed.

4.4 Acquisition of Single-Truck Data

Previously, in simulation, a PI controller tracking a constant velocity setpoint was used as a point of comparison, because a vehicle cruise controller was not available in simulation. This was used for the results outlined in chapters 2 and 3. One goal of acquiring single-truck data, was to have the truck drive over the route with its cruise controller in various settings. This captured real-world velocity profiles produced by different cruise controller settings. With the real-world cruise controller velocity profiles, a more appropriate quantification of fuel savings by Purdue strategies was made in simulation. Among many tuneable cruise control parameters, the most commonly adjusted is what is referred to as the "droop" settings. The droop settings of the cruise controller allow the vehicle velocity to deviate from the setpoint. An illustration of this for droop settings of ±3 MPH is shown in Figure 4.6.

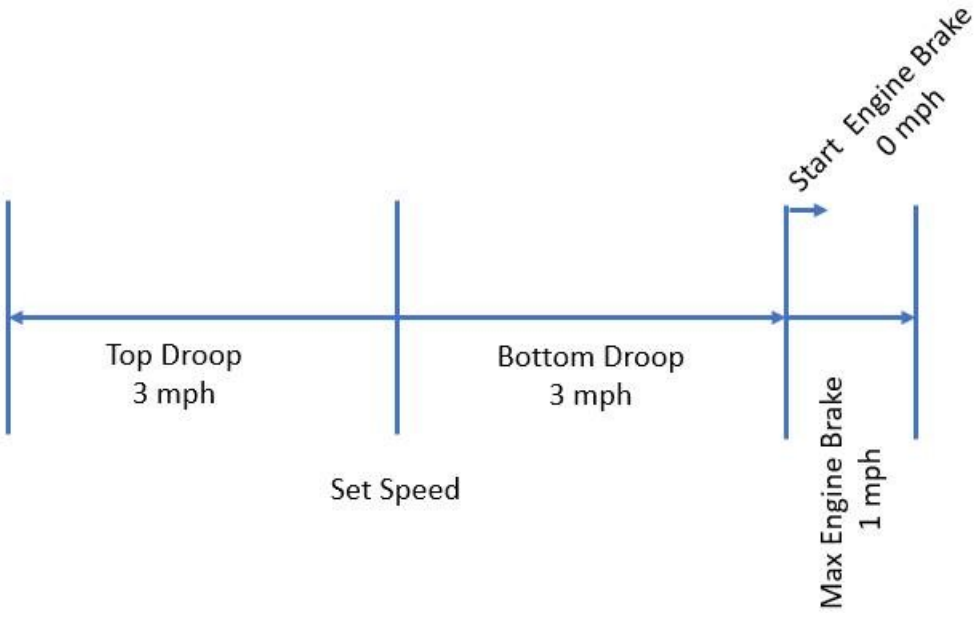

Fig. 4.6. Droop Illustration

Because this analysis was focused exclusively on the I-69 corridor, two trips were made to the south of Bloomington, IN, where the section of interest lies. The first trip successfully captured data for the Cummins cruise controller with the droop settings

set to ±0 MPH (no droop), and additionally, for droop settings set to +3.1/-6.1 MPH (max droop), which are the maximum values allowed by the Cummins software.

The second trip was a functionality check for the Purdue-developed LHPCC velocity profile. It allowed the Purdue team to gain insight into how well the truck would follow the commanded vehicle velocity, as well as yield an experimental velocity profile from an on-road truck. This, in turn, allowed for the use of experimental data to be run in the simulation framework. In a similar manner to wanting real-world cruise controller velocity profiles to move away from simulated constant-velocity profiles, having an experimental LHPCC profile provides a more accurate representation of LHPCC rather than continuing to rely only upon the high-fidelity vehicle model's prediction. The current state of the algorithm development, outlined in chapter 3, showed that a near-fixed gap platooning follow truck behind a lead truck with a route-optimized velocity profile yields the highest fuel savings. While the two-truck optimized velocity profile yielded slightly higher platoon average fuel savings in the predictive, two-truck, fixed gap high-fidelity vehicle model, than its single-truck counterpart (shown in Table 3.2), this algorithm takes longer to run than the single truck algorithm. Because the route had been slightly modified and a new optimal velocity profile needed to be generated, in the interest of time, the single-truck optimized algorithm was used to generate the velocity profile.

4.5 Experimental Data Results

Figure 4.7 plots the three experimental data samples from the single-truck testing (no droop, max droop, LHPCC) to explore how the truck behaved with each velocity tracking setting. The first subplot is road grade as a function of distance. The measured grade for the three tests align indicating that the rest of the measured parameters are also position aligned. This ensures a true "apples to apples" comparison. If there was misalignment of grade data, then it would not be appropriate to compare

how the vehicle speed, engine torque, retarder torque, and gear numbers differ from case to case.

The second subplot is vehicle velocity as a function of time. In this plot it can be seen that the trends in vehicle velocity for both no droop and max droop are very similar. As expected, the maximum and minimum velocities of the max-droop data yield more extreme values than those of the no-droop counterpart. Of particular interest is that the no-droop cruise controller still deviated very far from its 62 MPH setpoint, and that the max-droop cruise controller went both faster and slower than its respective upper and lower velocity limits; notably, the max-droop cruise controller had a peak velocity of around 70 MPH, which was about 5 MPH faster than expected. This was surprising because efforts were made to obey posted speed limits for I-69 testing. With a cruise control setpoint of 62MPH and a +3.1 MPH allowable deviation from the setpoint, a maximum velocity of 65.1 MPH was expected. The I-69 speed limit is 65 MPH, so the truck went 5 MPH faster than the I-69 speed limit. More specifically, according to the retarder settings, the retarder should have initiated when the truck reached 65.1 MPH (0 MPH over the speed threshold), and full retarder should have been in use when the truck reached 67.1 MPH (2 MPH over the speed threshold). In both cases, this did not appear to happen.

The third subplot is positive engine torque as a function of distance. A takeaway from this plot is that, as expected, the no-droop cruise controller saturates the engine torque much more frequently than the max-droop cruise controller and the LHPCC velocity profile.

The fourth subplot is engine retarder torque over position. Here it is seen that the LHPCC profile eliminated the use of the engine retarder, with the small exception of a quick use of retarder at the very end of the corridor. However, it is speculated that this was caused by a slow-moving vehicle that activated the truck's ACC. The reduction of engine retarder usage is significant because the use of the engine retarder equates to a loss of kinetic energy, which will quickly need to be regained by way of increased fueling. Avoiding usage of retarder, or friction brakes, should universally translate to

lower fuel consumption. The max-droop cruise controller was also able to minimize retarder use, and only used it in four instances. The no-droop cruise controller had significantly more retarder usage than both the max-droop cruise controller, and the LHPCC profile.

The fifth plot is of transmission gear number as a function of position. This shows that all three strategies operate primarily in top gear with a few instances of downshifts into 11th gear, and a single instance of downshifting into 10th gear in only the no-droop and LHPCC runs. The shift into 10th gear in the LHPCC profile aligns with the retarder usage; again, it is speculated that this was due to the ACC being activated. Additionally, the LHPCC profile had the fewest number of shifts, and the no-droop cruise controller had the most number of shifts while the max-droop cruise controller was between the two.

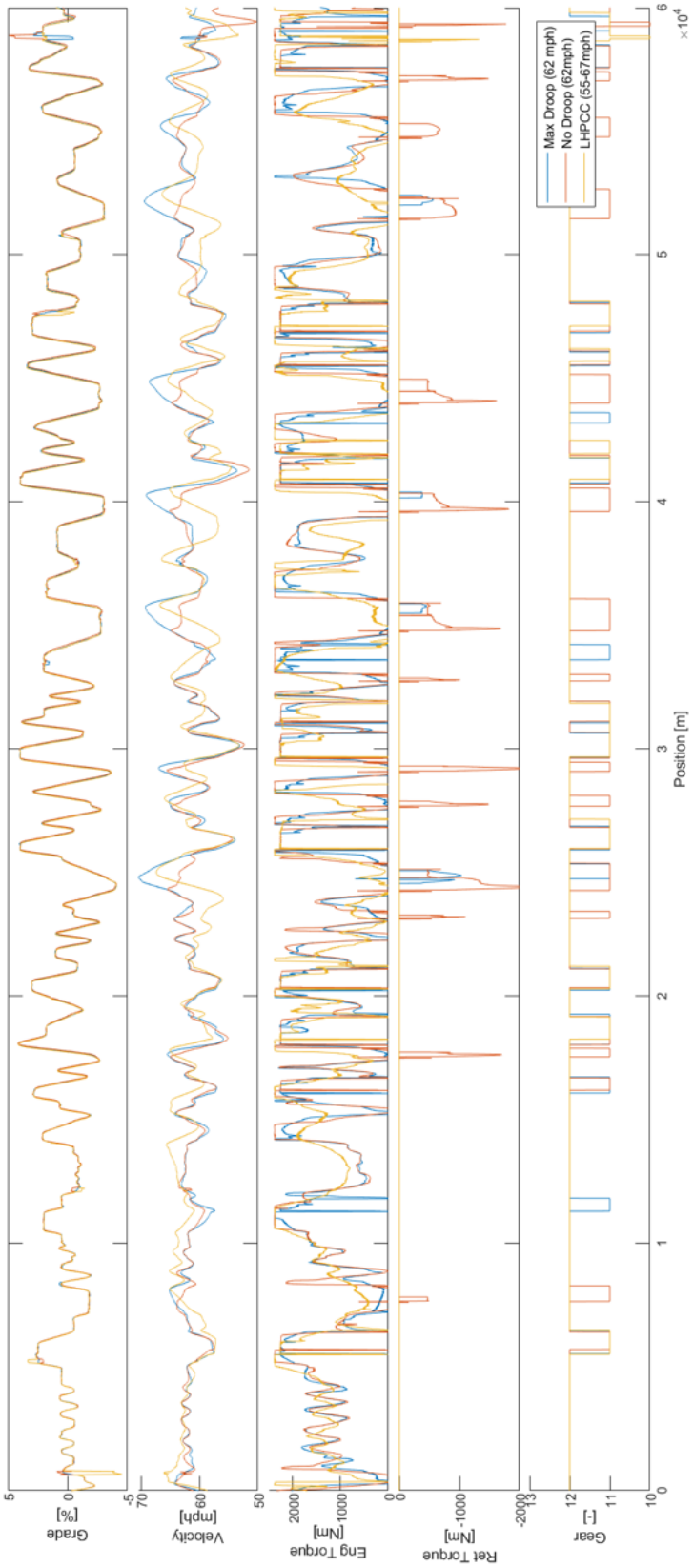

Fig. 4.7. Experimental Truck Results Over I-69

4.6 Simulation Results

The long-term goal of testing on I-69 is to experimentally confirm the fuel savings (predicted by simulation and the test cell) that could be realized over this corridor, with the expectation of fuel savings in excess of 12% (as discussed in chapter 3). The approach was to take the experimentally acquired velocity profiles and convert the data into the format that could be input into the high-fidelity vehicle model. Because of the inability to platoon, as previously mentioned due to SARS-CoV-2, a fixed gap platooning rear truck was unable to run behind the different lead vehicle velocity strategies. However, as shown in chapter 2, it is understood that fuel saving trends realized in simulation strongly align with fuel savings realized in the testbed, which utilizes the same engine in the Peterbilt 579 trucks. Additionally, because it was seen that the PI controller in the high-fidelity vehicle model tracks its desired velocity very closely, it is believed that the trends (percent savings) in fuel consumption numbers output from the high-fidelity vehicle model would very closely align with trends in real-world, on highway fuel consumption.

4.6.1 Single-Truck Simulation Results Using Experimental Velocity Profiles

After gathering the experimental velocity profiles, the data was put into the format that could be run in the high-fidelity vehicle model. The fuel consumption results, from the model, are shown in Table 4.1. The most rigid form of the cruise controller, no droop, was used as the point of comparison (in lieu of the previously used PI controller tracking a constant velocity) .

In Table 4.1, it can be seen that by only relaxing the cruise controller from no droop to max droop, a fuel savings of just over 6% can be realized. The Purdue-developed optimized velocity profile (LHPCC) saved 7.8%

Table 4.1.
Simulated Single Vehicles Using Experimental Data Over I-69

Profile	**Fuel Consumption [kg]**	**Savings [%]**
No Droop	17.56	-
Max Droop	16.50	6.0
Experimental LHPCC	16.19	7.8

4.6.2 Comparing Single-Truck Simulations: Predicted vs. Experimental Velocity Profiles

To give further insight into how the vehicle responded when tracking the LHPCC velocity profile, Figure 4.8 compares the experimental data from the experimental LHPCC shown in Figure 4.7 to the data, for the same parameters, from the LHPCC high-fidelity vehicle model's prediction.

As in Figure 4.7, the first subplot in Figure 4.8 is of grade as a function of distance to ensure an accurate comparison. The second plot shows vehicle velocity with an additional inclusion of commanded velocity in order to check the tracking of both the simulation as well as the on-road truck. In this plot, it can be seen that the simulation tracked the commanded velocity almost perfectly with a few small deviations. The on-road truck also appears to have tracked the velocity very well, but without the perfection of the simulation, which was expected. There was a relatively large deviation at the very end of the corridor; it is, again, speculated that this was due to a slow-moving vehicle triggering the ACC and slowing the truck down, not due to a problem with the testing equipment.

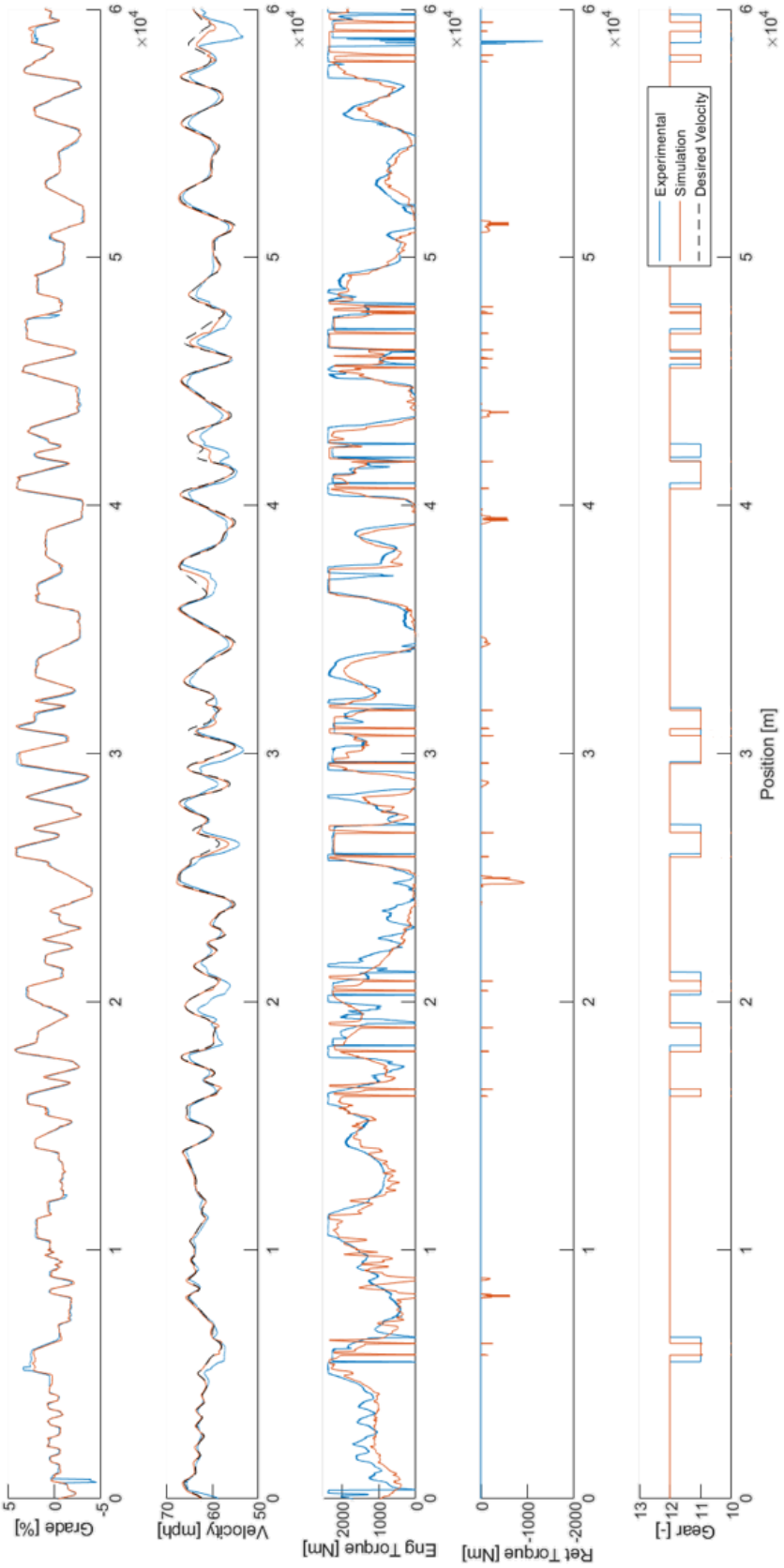

Fig. 4.8. Experimental and Simulation LHPCC Comparison

An interesting aspect, when comparing the original simulation to the simulation of the experimental data, is that when the high-fidelity vehicle model tracked the desired optimized velocity profile, its predicted fuel consumption was higher than when the high-fidelity model tracked the experimental velocity of the truck attempting to follow the optimized velocity profile. This difference appears to be largely attributable to the near elimination of retarder torque in the case of the experimental profile. These results are shown in Table 4.2

Table 4.2.
LHPCC Fuel Savings Comparison Over I-69

Profile	**Fuel Consumption [kg]**	**Percent Savings [%]**
No Droop	17.56	-
Simulation LHPCC	16.66	5.1
Experimental LHPCC	16.19	7.8

While this discovery was definitely more pleasant than the opposite situation (if the experimental velocity profile had consumed more fuel), it indicated that the velocity profile generated by the simple model optimizer was not quite the most optimal due to the limitations of the simple model not fully capturing all real-world phenomena. This decreased fuel consumption was likely due to various vehicle dynamics (e.g., shifting) that were not accounted for in the optimized profile, but were encountered in the high-fidelity vehicle model. Another possible explanation is that there was a small discrepancy in trip time. The prediction from the high-fidelity vehicle model finished the route 10 seconds faster than the experimental profile. This could have accounted for some slight increase in fuel consumption in the high-fidelity prediction, but it most likely is not responsible for the majority of the difference, as it is less than a 0.5% difference in trip time.

4.6.3 Platoon Simulation Results Using Experimental Velocity Profiles

Using the same experimental velocity profiles in simulation and adding a (simulated) fixed gap platooning rear truck, fuel consumption values were obtained and are shown in Table 4.3. Just as in Table 4.1, the percent savings were relative to a single vehicle using a droop cruise controller (17.56 kg).

Table 4.3.
Simulated Platoon Using Experimental Data Over I-69

Velocity Profile	**Lead [kg]**	**Follow [kg]**	**Platoon Avg. [kg]**	**Savings [%]**
No Droop	17.26	17.56	17.41	0.9
Max Droop	16.17	16.34	16.26	7.4
Experimental LHPCC	15.85	15.45	15.65	10.9

One interesting discovery in the platooning data was that in the case where the lead vehicle was using a no-droop cruise controller, the standard PlatoonPro follow truck saved no fuel compared to the baseline single truck, and it also consumed more than the lead truck in the platoon. Upon further investigation, it was determined that the follow truck did indeed have a reduction in aerodynamic drag, but following a lead truck with a relatively stiff cruise controller made tracking more difficult and increased the retarder usage. The integrated retarder usage increased from 34.71 MJ (single truck no droop) to 54.34 MJ. When the rear truck uses its retarder, it effectively transfers its kinetic energy to heat. The kinetic energy is essentially derived from the fuel, so by increasing the retarder usage, the follow truck is wasting its fuel.

It was previously discovered that simultaneous shifting (SS) occasionally yields lower fuel consumption than its non-simultaneous shifting counterparts. However, more importantly, simultaneous shifting allows for the rear truck to more adequately manage the gap growth to discourage cut-ins. Table 4.4 explores the fuel consumption

of a platoon when simultaneous shifting of the lead and follow trucks was being used. Again, the percent savings were relative to a single truck using a no-droop cruise controller (17.56 kg).

Table 4.4.
Simulated Platoon with SS Using Experimental Data Over I-69

Velocity Profile	**Lead [kg]**	**Follow [kg]**	**Platoon Avg. [kg]**	**Savings [%]**
No Droop	17.26	17.42	17.34	1.3
Max Droop	16.17	16.39	16.28	7.3
Experimental LHPCC	15.85	15.32	15.58	11.3

The results shown in Table 4.4 confirm previous research results that showed simultaneous shifting does not having a large impact on fuel savings. It did, however, slightly improve both the no-droop cruise control case as well as the LHPCC by 0.4%. This data now indicates that the largest fuel savings that can be expected over I-69, using two trucks, is around 11.3%.

As previously mentioned, the main benefit of simultaneous shifting is gap management to avoid cut-ins. The maximum simulated platoon gap for each strategy both with and without simultaneous shifting is explored in Table 4.5. The interesting aspect of the gap data is that in the case of LHPCC with simultaneous shifting, the gap was reduced to about 23 meters, which is significantly lower than in the max-droop case of 31 meters. This is important because even though max droop might have close to the same benefits when it comes to fuel savings, it appears to still be relatively hard to follow with a fixed gap platooning rear truck even when simultaneous shifting is used.

Table 4.5.
Maximum Simulated Platoon Gap Using Experimental Data Over I-69

Velocity Profile	**Without SS [m]**	**With SS [m]**
No Droop	50.90	35.21
Max Droop	41.88	31.28
Experimental LHPCC	33.85	23.02

4.6.4 Comparing Platoon Simulations: Predicted vs. Experimental Velocity Profiles

In subsection 4.6.3 the experimental LHPCC velocity profile was given a simulated fixed gap platooning follow vehicle. It was then compared to both no-droop and max-droop velocity profiles, which were also given fixed gap platooning follow vehicles. Additionally, in subsection 4.6.2 the experimental LHPCC single truck was compared to the predicted, simulated LHPCC single truck. This subsection further investigates the differences between the experimental and predicted LHPCC fuel consumption, but now with simulated fixed gap platooning rear trucks both with and without simultaneous shifting. To reiterate, all savings percentages are with respect to a single truck using a no-droop cruise controller.

Table 4.6.
Simulated LHPCC Platoon Fuel Savings Comparison Over I-69

Velocity Profile	**Lead [kg]**	**Follow [kg]**	**Platoon Avg. [kg]**	**Savings [%]**
Simulated LHPCC	16.31	15.58	15.94	9.2
Experimental LHPCC	15.85	15.45	15.65	10.9

In Table 4.6, the platoon lead saved more fuel when following the experimental LHPCC profile than the desired LHPCC profile, similar to the single-truck case shown in Table 4.2. This was expected because trends in the platoon lead's fuel consumption very closely follow trends in the single vehicle fuel consumption (as their velocity profiles are the same). Additionally, as intuition might suggest, the follow vehicle fuel consumption is also lower when following the velocity of the experimental LHPCC than it is when following the desired LHPCC profile.

Table 4.7 is the same as Table 4.6, but with the addition of simultaneous shifting. Comparing the percent savings from the two tables confirms that simultaneous shifting, again, does not universally have a significant impact on fuel consumption.

Table 4.7.
Simulated LHPCC Platoon with SS Fuel Savings Comparison Over I-69

Velocity Profile	**Lead [kg]**	**Follow [kg]**	**Platoon Avg. [kg]**	**Savings [%]**
Simulated LHPCC	16.31	15.52	15.92	9.4
Experimental LHPCC	15.85	15.32	15.58	11.3

The maximum simulated platoon gaps are shown in Table 4.8

Table 4.8.
Maximum Simulated Platoon Gap LHPCC Comparison Over I-69

Velocity Profile	**Without SS [m]**	**With SS [m]**
Simulated LHPCC	42.83	27.01
Experimental LHPCC	33.85	23.02

4.6.5 Relaxing the Predictive Cruise Controller

While the most obvious benefit of LHPCC over the max-droop cruise controller was its increase in fuel savings, there are a number of other benefits to consider when comparing these two strategies. These include better gap management and more authority over vehicle speed (to ensure the speed limit is not broken). This subsection aims to target the issue of the max-droop cruise controller going 5 miles per hour over its allowed maximum speed.

The benefit of LHPCC is that it can optimize the velocity profile such that it can speed up and slow down at various points in the corridor to minimize engine retarder (and/or friction brakes), which oftentimes is an unnecessary transfer of kinetic energy into heat rejected to the environment. If the max-droop cruise controller allowed the truck to reach speeds of 70 miles per hour, then the best "apples to apples" comparison with LHPCC was to allow the optimizer to also permit the truck to reach up to 70 miles per hour.

Table 4.9 shows predicted, simulated fuel consumption results for a new relaxed LHPCC velocity profile that allowed the truck to reach up to 70 miles per hour (denoted relaxed LHPCC). Table 4.10 shows the same strategies with simultaneous shifting on the rear truck.

Table 4.9.
Relaxed LHPCC Simulated Platoon Comparison Over I-69

Velocity Profile	**Lead [kg]**	**Follow [kg]**	**Platoon Avg. [kg]**	**Savings [%]**
Simulated LHPCC	16.31	15.58	15.94	9.2
Relaxed LHPCC	15.73	15.22	15.47	11.9
Max Droop	16.17	16.34	16.26	7.4

Table 4.10.
Relaxed LHPCC Simulated Platoon with SS Comparison Over I-69

Velocity Profile	**Lead [kg]**	**Follow [kg]**	**Platoon Avg. [kg]**	**Savings [%]**
Simulated LHPCC	16.31	15.52	15.92	9.4
Relaxed LHPCC	15.73	15.18	15.45	12.0
Max Droop	16.17	16.39	16.28	7.3

It is important to remember that both LHPCC strategies shown in Tables 4.9 and 4.10 are based on the values from simulation results only, and the max droop values are from the real-world velocity profile being rerun in simulation. While this is a bit of an "apples to oranges" comparison, there is the unifying fact that both velocity profiles were being fed into the same high-fidelity vehicle model, and it was the best that could be done with the restrictions that were on testing.

Table 4.11 shows the simulated maximum platoon gap over the corridor for each strategy both with and without simultaneous shifting.

Table 4.11.
Maximum Simulated Relaxed LHPCC Platoon Gap Over I-69

Velocity Profile	**Without SS [m]**	**With SS [m]**
Simulated LHPCC	42.83	27.01
Relaxed LHPCC	32.78	24.65
Max Droop	41.88	31.28

An astute observer would recall that in subsections 4.6.2 and 4.6.4, when comparing the simulation prediction vs. simulated on-road truck velocity profiles, the simulated on-road fuel consumption was lower than the simulation prediction. While it was desirable to run the relaxed version of the LHPCC on the single truck, SARS-

CoV-2 prevented this from happening, and any assumptions about the behavior of the real-world truck versus the predicted relaxed LHPCC will be avoided.

Additionally, another way to more fairly compare the original LHPCC profile to the max-droop cruise controller would have been to set the velocity setpoint for the cruise controller at a lower speed. A setpoint of 57 MPH was considered as it was 5 MPH slower than the previously used setpoint, and should, theoretically, reduce the maximum speed by 5 MPH (from 70 MPH down to the speed limit of 65 MPH). Again, due to SARS-CoV-2, no further vehicle testing was possible.

4.7 Summary

Truck data over I-69 was taken with no-droop and max-droop cruise control settings as well as with an LHPCC profile. Many important observations were made such as the fact that even when the cruise controller was in its most rigid calibration (i.e., no droop), the velocity of the truck still deviated from its setpoint by a couple of miles per hour (which was not the case for the PI controller tracking a constant velocity used as a point of comparison in chapters 2 and 3). With max droop, velocities no slower than 55.9 MPH and no faster than 65.1 MPH were expected based on the calibration settings. However, the measured max-droop minimum speed was 53 MPH (2 MPH slower than its minimum expected value), and its maximum speed was about 70 MPH (5 MPH over its maximum expected value). When the experimental velocity traces are run in simulation, the LHPCC profile yields lower fuel consumption numbers than both the no-droop and max-droop velocity profiles. This is true for all possible scenarios: single truck, platoon lead and follow, and platoon lead and follow with simultaneous shifting. The case that saves the most fuel is a lead truck using an LHPCC velocity profile with a follow truck using PlatoonPro with simultaneous shifting. The platoon average savings are 11.3% relative to a single truck using a no-droop cruise controller. In addition to more fuel savings, there are two other benefits to LHPCC. First, it does a better job of reducing the maximum platoon gap,

especially with the use of simultaneous shifting. When using max droop as a lead truck profile, an unexpected result was that the platoon gap grew to greater than 30 meters, even with simultaneous shifting. Second, LHPCC is able to track its desired velocity very well, which, in turn, means that it should not excessively break the speed limit like the max-droop case did. While it would be possible to potentially lower the max-droop setpoint by 5 miles per hour to theoretically reduce its top speed by 5 MPH (back down to 65 MPH), this would likely cause a significant increase in trip time (a very undesirable outcome).

5. SUMMARY AND FUTURE WORK

5.1 Summary

Saving fuel on class 8 trucks could have a large impact on the reduction of greenhouse gas emissions as well as decreasing trucks' operating costs. Different algorithms and control strategies have been developed to realize fuel savings, and were tested on an engine test cell to check for feasibility of real-world implementation and real-world effectiveness. Additionally, a two-truck optimized platoon algorithm was developed to yield the highest fuel savings possible from vehicle level optimization. Lastly, a Peterbilt 579 was driven over a portion of I-69 to collect real-world vehicle behavior over this corridor. The two main takeaways are 1) there is improved fuel savings when the lead truck is operated more efficiently either with LHPCC (best case) or a max-droop cruise controller, and 2) gap management (which allows for platooning over graded terrain) can be improved with simultaneous shifting, lead truck LHPCC, or max-droop cruise control settings on the lead truck (in that order of positive impact).

Test cell #2 at Purdue's Herrick Laboratories houses a Cummins X15 Efficiency Series Engine. This engine was used to validate Purdue developed algorithms by calculating fuel consumption and demonstrating that the simulation model predicted reasonable engine torque response dynamics. One strategy confirmed a fuel savings of 5.38% over a section of I-69, and another strategy confirmed a fuel savings of 13.11% over I-280. The testbed consistently produced fuel consumption data with standard deviation values of less than 0.11 lbs. of fuel, and appeared to be incredibly repeatable.

Significant fuel savings on class 8 trucks can be had both from platooning and route optimized velocity profiles. While these strategies had previously been combined, an optimizer had never been given control over both vehicles' velocities simultaneously.

A framework for a two-truck MPC controller was developed and after exercising it over two different corridors (a section of I-280 and a section of I-69), it revealed that given the problem formulation, the most optimal behavior of two vehicles is to optimize a velocity profile for the lead truck such that a follow truck can easily maintain a fixed gap behind the lead truck so both trucks can reap the full benefits of platooning. Doing this yielded a combined (averaged) fuel savings of around 14% over I-280 and around 12% over I-69.

Lastly, a Peterbilt 579 was driven over the section of I-69 that was used for analysis throughout this thesis. Datasets for a no-droop and max-droop cruise controller were taken as well as a dataset for a Purdue-developed LHPCC variable velocity profile. The experimental velocity profile was then run in simulation with a platooning follow truck, and yielded savings of 11% relative to a simulated no-droop single truck. Additionally, when the follow truck was behind a lead truck utilizing the LHPCC profile and simultaneous shifting, the maximum gap was reduced to 23 meters from over 50 meters when the follow truck was following the no-droop lead without simultaneous shifting.

5.2 Recommendations for Future Work

This thesis has shown that significant fuel savings are attainable through the use of advanced platooning strategies, but more testing and development is needed.

The test cell has proven itself to be an incredibly useful and repeatable tool. However, some tests deviated from their predicted fuel consumption more than others. Continuing to update and refine models, by running tests at steady states, could allow for the calculation of BSFC to see if there are specific operating conditions in the model that differ from the operating conditions on the testbed.

The two-truck MPC algorithm has consistently yielded near-fixed gap platooning distance to be most optimal behind an optimized lead truck. Further exercising of the model over more heavily graded routes, could show that more gap flexibility is

desirable on grades above 5%. Additionally, attempting to relax the speed constraint (as may be feasible in a dedicated class 8 truck platooning lane) to completely eliminate the retarder torque over the section of I-280 could likely yield significantly higher fuel savings. Lastly, capturing more vehicle dynamics into the solver (e.g., shifting), could translate into velocity profiles that consume even less fuel.

Furthermore, for truck testing, doing full J1321 fuel economy testing (both single-truck and two-truck) to get concrete evidence for the proposed fuel savings is an important step in understanding the real-world fuel economy benefits. Finally, running the relaxed LHPCC profile on a truck would allow for a more "apples to apples" comparison of LHPCC to max droop to further understand the benefits of LHPCC over max droop.

REFERENCES

REFERENCES

[1] ExxonMobil, "Outlook for energy: A persepective to 2040," 2019. [Online]. Available: https://corporate.exxonmobil.com/Energy-and-environment/Looking-forward/Outlook-for-Energy/Outlook-for-Energy-A-perspective-to-2040#ExxonMobilsupportstheParisAgreement

[2] United States Environmental Protection Agency, "Inventory of u.s. greenhouse gas emissions and sinks," 2018. [Online]. Available: https://www.epa.gov/ghgemissions/inventory-us-greenhouse-gas-emissions-and-sinks

[3] ——, "Fast facts on transportation greenhouse gas emissions," 2017. [Online]. Available: https://www.epa.gov/greenvehicles/fast-facts-transportation-greenhouse-gas-emissions

[4] United States Department of Energy, "Maps and data - average annual fuel use by vehicle type," 2020. [Online]. Available: https://afdc.energy.gov/data/

[5] J. Endres, "Want to optimize your fleet? know your average trucking cost per mile," 2018. [Online]. Available: https://www.paragonrouting.com/en-us/blog/post/want-optimize-your-fleet-know-your-average-trucking-cost-mile/

[6] Indiana Department of Transportation, "2014 multimodal freight and mobility plan," 2014. [Online]. Available: https://www.in.gov/indot/2513.htm

[7] National Research Council, *Vehicle Technologies for Reducing Load-Specific Fuel Consumption*. The National Academies Press, 2010, pp. 91–92. [Online]. Available: https://doi.org/10.17226/12845

[8] RTS Carrier Services. (2019) How better aerodynamics lead to fuel savings. [Online]. Available: https://www.rtscarrierservices.com/article/how-better-aerodynamics-lead-fuel-savings

[9] The Breakthrough Blog. (2017) Why we're investing in the future of transportation and fuel efficiency. [Online]. Available: https://www.breakthroughfuel.com/blog/peloton-future-transportation/

[10] M. Lammert, K. Kelly, and J. Yanowitz, "Correlations of platooning track test and wind tunnel data," National Renewable Energy Laboratory, Golden, CO, Tech. Rep., 2018.

[11] Peloton Technoloty. (2020) Platooning combines advanced technologies to improve safety and fuel efficiency. [Online]. Available: https://peloton-tech.com/how-it-works/

[12] M. Lammert, A. Duran, J. Diez, K. Burton, and A. Nicholson, "Effect of platooning on fuel consumption of class 8 vehicles over a range of speeds, following distances, and mass," *SAE Int. J. Commer. Veh*, vol. 7, pp. 626–639, 2014.

[13] "Electronic drawbar - digital innovation project report - presentation of the results," MAN Truck and Bus, DB Schenker and the Hochschule Fresenius, Tech. Rep., 2019.

[14] M. Lammert, B. Bugbee, Y. Hou, A. Mack, M. Muratori, J. Holden, A. Duran, and E. Swaney, "Exploring telematics big data for truck platooning opportunities," in *SAE World Congress Experience*. SAE International, 2018.

[15] G. Wood. (2020) Truck platooning expected to make inroads in 2020. [Online]. Available: https://www.oemoffhighway.com/electronics/smart-systems/automated-systems/article/21114230/truck-platooning-expected-to-make-inroads-in-2020

[16] I. Ibitayo, "Enhanced class 8 truck platooning via simultaneous shifting and model predictive control," August 2019.

[17] J. Foster, "Advanced control strategies for diesel engine thermal management and class 8 truck platooning," August 2020.

[18] A. Taylor, "Diesel engine air handling strategies for fuel efficient aftertreatment thermal mangagement & connected and automated class 8 trucks," Ph.D. dissertation, Purdue University - West Lafayette, December 2018.

[19] K. Salari, "Doe's effort to improve heavy vehicle fuel efficiency through improved aerodynamics overview: Llnl-pres-688057," U.S. Department of Energy by Lawrence Livermore National Laboratory, Washington, D.C., Tech. Rep., 2016.